The method of fundamental solutions for potential, Helmholtz and diffusion problems

M.A. Golberg[1] & C.S. Chen[2]
[1] *2025 University Circle, Las Vegas, NV 89119, U.S.A.*
[2] *Department of Mathematical Sciences, University of Nevada, Las Vegas, NV 89154, U.S.A.*
EMail: chen@nevada.edu

Abstract

We survey some recent developments in the application of the method of fundamental solutions for the numerical solution of elliptic and parabolic partial differential equations. Of particular interest are the extensions of the method to solve inhomogeneous and nonlinear boundary value problems and time dependent problems through the use of the Laplace transform. We discuss a number of convergence results for Laplace's equation in the plane and extend these to establish convergence results for Poisson's equation when the source term is approximated by radial basis functions. Numerical results are presented showing the efficiency and stability of the method.

1 Introduction

In the traditional boundary element method (BEM) solutions of partial differential equations (PDEs) are represented by layer potentials on the surface of the domain and using various limiting properties of these potentials one arrives at integral equations for the determination of their densities [1, 2]. Solving these equations numerically provides a powerful tool for the solution of numerous scientific and engineering problems [1, 2]. With hundreds of papers being published each year on this technique [3], it has become established as

one of the basic computational tools in engineering analysis and a viable alternative to the finite element and finite difference methods (FEMs and FDMs). Despite its popularity, there are many problems related to its efficient implementation. Among these are difficulty in meshing surfaces, particularly in three dimensions (3D) [4], the need to compute complicated singular integrals [2, 4, 5] and the often slow convergence due to the use of low order polynomial approximations [1, 2]. As a consequence, it is of some interest to develop methods which would alleviate these problems. One technique for doing this is to represent solutions using layer potentials on surfaces which are not the physical surfaces. This method, often called the *regular* BEM [6], does not require complicated meshing and avoids the problem of evaluating singular integrals. When these potentials are discretized, one arrives at representations of the solution in terms of fundamental solutions of the given partial differential equation (PDE). In this form the method is known as the *Method of Fundamental Solutions* (MFS) and can be a highly efficient alternative to the traditional BEM [7-13]. (The method is also known by many other names in the literature. Among these are the *superposition method* [13], *desingularized method* [14], and the *charge simulation method* (CSM) [15].)

In this chapter we discuss some recent work on the application of the MFS to solve Laplace's, Poisson's, Helmholtz's and diffusion equations in $\mathbb{R}^2$ and $\mathbb{R}^3$ and expand on material developed in [2]. Of particular interest are some new convergence results for the MFS for Laplace's and Poisson's equations in $\mathbb{R}^2$ and extensions of the method to solve time-dependent problems [16].

The paper is divided into six sections. In Section 2 we review past work on the MFS for Laplace's equation and discuss some convergence results of Katsurada and Okamoto [17] and Katsurada [18] which extends the previous work of Cheng [19] who studied the convergence of the MFS on circular domains in $\mathbb{R}^2$. This work is important in that it lends further support to the conjecture that for smooth solutions the convergence of the MFS is exponential (spectral) and improves the farther the source surface is from the physical one. In addition, the work of Kitigawa [20, 21] gives some guidance as to when the ill-conditioning of the MFS equations can cause numerical difficulties. This has been one of the perplexing problems of the method [2, 22]. We also discuss the work of Karageorghis et al on using singular solutions to solve mixed boundary value problems on domains in $\mathbb{R}^2$

with corners [2].

In Section 3 we examine some applications of the MFS to solve the Helmholtz equation. In contrast to Laplace's equation, where interior problems are usually of most interest, for the Helmholtz equation the problems of most interest are exterior problems resulting from the scattering of acoustic and electromagnetic waves from surfaces [13]. This problem is difficult to solve by standard BEMs because solutions to the layer equations are not unique [23]. On the other hand, the MFS seems to be free of such complications which is an additional motivation for its further investigation [13].

In Section 4 we extend the MFS technique to solve Poisson's equation and we report on some recent experiments comparing the MFS with several more traditional BEMs.

In Section 5 we consider an approach to solving the diffusion equation using the MFS. Here we proceed along the lines of Zhu et al [24] who used the Laplace transform and standard BEMs (See Chapter 1). Rather than using time-dependent potentials [25], we remove the time dependence by using the Laplace transform, solve the resulting elliptic problem by the MFS and then numerically invert the transform to obtain the time dependent solution.

When the initial condition for the diffusion equation is not harmonic, the time-independent problem is inhomogeneous. As for Poisson's equation, this requires that one be able to calculate particular solutions for a Helmholtz-type equation. In [16] this was done by numerical integration to evaluate a generalization of Atkinson's formula [2]. More recently, the authors and Rashed [26] have discovered analytic formulas for particular solutions when the inhomogeneous term is a thin plate spline (TPS) or higher order splines. This opens an approach to the efficient solution of inhomogeneous Helmholtz-type equations both for the MFS and standard BEMs. We close with some directions for future research.

2 The MFS for Laplace's equation

2.1 Derivation

To illustrate the basic ideas of the MFS we consider the solution of the interior Dirichlet problem for Laplace's equation in $\mathbb{R}^d, d = 2, 3$. For this, let D be a bounded, connected, simply connected domain in $\mathbb{R}^d$ with boundary S and consider solving the boundary value problem

(BVP)

$$\begin{aligned} \Delta u(\mathbf{P}) &= 0, \quad \mathbf{P} \in D, && (1) \\ u(\mathbf{P}) &= g(\mathbf{P}), \quad \mathbf{P} \in S, && (2) \end{aligned}$$

where g is a known function. As is well known, when S is sufficiently smooth (generally Lipschitz continuous) Eqn. (1) - Eqn. (2) has a unique solution [2]. Because of its practical importance, numerous numerical techniques have been proposed for solving Eqn. (1) - Eqn. (2). Among these are the FEM, FDM, spectral methods [27] and the BEM [1, 2]. For the latter, the traditional approach has been to represent u in terms of the *double layer potential*

$$u(\mathbf{P}) = \int_S \frac{\partial G(\mathbf{P}, \mathbf{Q})}{\partial n_{\mathbf{Q}}} \sigma(\mathbf{Q}) ds, \quad \mathbf{P} \in D, \tag{3}$$

where σ is the unknown density and

$$G(\mathbf{P}, \mathbf{Q}) = \begin{cases} \dfrac{1}{2\pi} \log \|\mathbf{P} - \mathbf{Q}\|, & (\mathbf{P}, \mathbf{Q}) \in \mathbb{R}^2, \\ \dfrac{-1}{4\pi \|\mathbf{P} - \mathbf{Q}\|}, & (\mathbf{P}, \mathbf{Q}) \in \mathbb{R}^3, \end{cases} \tag{4}$$

is the *fundamental solution* of Δ. Taking the limit $\mathbf{P} \to S$ leads to a Fredholm integral equation of the second kind for σ [2]. More recently, various authors have considered using the single layer representation [2, 28, 29]

$$u(\mathbf{P}) = \int_S G(\mathbf{P}, \mathbf{Q}) \sigma(\mathbf{Q}) ds, \quad \mathbf{P} \in D, \tag{5}$$

which gives the equation

$$\int_S G(\mathbf{P}, \mathbf{Q}) \sigma(\mathbf{Q}) ds = g(\mathbf{P}), \quad \mathbf{P} \in S, \tag{6}$$

for σ. Discretization of Eqn. (6) often gives efficient algorithms for solving Eqn. (1) - Eqn. (2) [2, 28, 29].

To overcome problems with evaluating the singular integrals in Eqn. (6) and the meshing of S, an alternative approach to solving Eqn. (1) - Eqn. (2) analogous to Eqn. (5), represents the solutions as

$$u(\mathbf{P}) = \int_{\hat{S}} G(\mathbf{P}, \mathbf{Q}) \sigma(\mathbf{Q}) ds, \quad \mathbf{P} \in D, \tag{7}$$

where $\hat{S}$ is the surface of a domain $\hat{D}$ containing D.

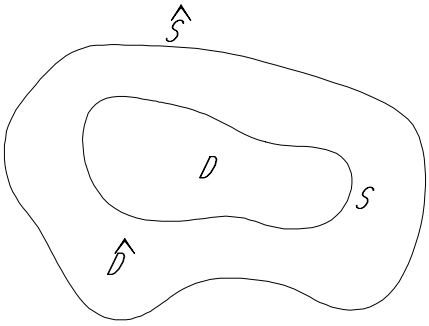

Figure 1. Geometry for the MFS.

It is easily verified that $\Delta u = 0$. To satisfy the boundary condition in Eqn. (2), let $\mathbf{P} \to S$ giving

$$\int_{\hat{S}} G(\mathbf{P}, \mathbf{Q})\sigma(\mathbf{Q})ds = g(\mathbf{P}), \quad \mathbf{P} \in S, \tag{8}$$

to determine $\sigma(\mathbf{Q}), \mathbf{Q} \in \hat{S}$. Solving Eqn. (8) numerically for σ and substituting the solution into Eqn. (6) gives a numerical technique for solving Eqn. (1) - Eqn. (2) once $\hat{S}$ has been determined. This method is often called the *regular* BEM in the engineering literature [6].

Assuming $\hat{S}$ is known, one can solve Eqn. (8) by techniques analogous to those for Eqn. (6). For example, suppose $\{\varphi_j(\mathbf{Q})\}_1^\infty$ is a complete set of functions on $\hat{S}$, then we approximate σ by

$$\sigma_n(\mathbf{Q}) = \sum_{j=1}^{n} c_j \varphi_j(\mathbf{Q}), \quad \mathbf{Q} \in \hat{S}. \tag{9}$$

Substituting Eqn. (9) into Eqn. (8) and collocating at n points on $\{\mathbf{P}_k\}_1^n$ on S gives

$$\sum_{j=1}^{n} c_j \int_{\hat{S}} G(\mathbf{P}_k, \mathbf{Q})\varphi_j(\mathbf{Q})ds = g(\mathbf{P}_k), \quad 1 \le k \le n, \tag{10}$$

to determine $\{c_j\}_1^n$. In general, the integrals

$$\int_{\hat{S}} G(\mathbf{P}_k, \mathbf{Q})\varphi_j(\mathbf{Q})ds, \quad 1 \le j \le n, \tag{11}$$

have to be calculated numerically. Since $\mathbf{P}_k \neq \mathbf{Q}$,$1 \leq k \leq n$, the integrand $G(\mathbf{P}_k, \mathbf{Q})$ is nonsingular, so that standard quadrature rules can be used to approximate Eqn. (11) giving

$$\int_{\hat{S}} G(\mathbf{P}_k, \mathbf{Q})\varphi_j(\mathbf{Q})ds \simeq \sum_{l=1}^{M} w_l G(\mathbf{P}_k, \mathbf{Q}_l)\varphi_j(\mathbf{Q}_l) \tag{12}$$

Substituting Eqn. (12) into Eqn. (10) gives $\{\hat{c}_j\}_1^n$, the approximations to $\{c_j\}_1^n$, as the solutions to

$$\begin{aligned} & \sum_{j=1}^{n} \hat{c}_j \left[\sum_{l=1}^{M} w_l G(\mathbf{P}_k, \mathbf{Q}_l)\varphi_j(\mathbf{Q}_l) \right] \\ = & \sum_{l=1}^{M} w_l \left[\sum_{j=1}^{n} \hat{c}_j \varphi_j(\mathbf{Q}_l) \right] G(\mathbf{P}_k, \mathbf{Q}_l) = g(\mathbf{P}_k), \quad 1 \leq k \leq n. \end{aligned} \tag{13}$$

Letting

$$b_l = \sum_{j=1}^{n} \hat{c}_j \varphi_j(\mathbf{Q}_l) \tag{14}$$

Eqn. (13) becomes

$$\sum_{l=1}^{M} a_l G(\mathbf{P}_k, \mathbf{Q}_l) = g(\mathbf{P}_k), \quad a_l = w_l b_l, \quad 1 \leq k \leq n. \tag{15}$$

If $M = n$, the *discrete regular* BEM in Eqn. (15) is equivalent to approximating the solution to Eqn. (1) by

$$u_n(\mathbf{P}) = \sum_{j=1}^{n} a_j G(\mathbf{P}, \mathbf{Q}_j), \quad \mathbf{Q}_j \in \hat{S} \tag{16}$$

and satisfying Eqn. (2) by setting

$$u_n(\mathbf{P}_k) = g(\mathbf{P}_k), \quad 1 \leq k \leq n. \tag{17}$$

We refer to the representation in Eqn. (16) as the MFS. This equivalence between the regular BEM and the MFS seems to have been overlooked in the literature [6].

Although Eqn. (16) follows naturally from Eqn. (7) in $\mathbb{R}^3$, we generally need to add a constant to Eqn. (16) in $\mathbb{R}^2$ for completeness purposes [22]. In this case we use

$$u_n(\mathbf{P}) = \sum_{j=1}^{n} a_j G(\mathbf{P}, \mathbf{Q}_j) + c, \tag{18}$$

and collocate at $n+1$ points $\{\mathbf{P}_k\}_1^{n+1}$ on S giving

$$\sum_{j=1}^{n} a_j G(\mathbf{P}_k, \mathbf{Q}_j) + c = g(\mathbf{P}_k), \quad 1 \le k \le n+1. \tag{19}$$

When S is a circle, we can generally take $c = 0$. Numerical examples demonstrating the efficiency of this method are given in [2, 7-12, 22].

Observe that in using Eqn. (16) or Eqn. (18) neither boundary meshing nor numerical integration is required. Moreover, when S and g are smooth u_n often converges exponentially to u so that in contrast to usual BEMs the system of equations given by Eqn. (17) or Eqn. (19) is usually small, often $n \le 30$ suffices in $\mathbb{R}^2$ and $n \le 100$ in $\mathbb{R}^3$ [11].

A further advantage of the MFS over the BEM is that the accuracy of the MFS does not deteriorate near the boundary S as is common in the BEM [2].

Although we have introduced the MFS in terms of the Dirichlet problem, quite arbitrary boundary conditions, both linear and nonlinear [2, 10], can be incorporated in the MFS with no more difficulty. For example, a common situation is to have mixed boundary conditions on S of the form

$$u(\mathbf{P}) = g_1(\mathbf{P}), \quad \mathbf{P} \in S_1, \tag{20}$$

$$\frac{\partial u(\mathbf{P})}{\partial n_{\mathbf{P}}} = g_2(\mathbf{P}), \quad \mathbf{P} \in S_2, \tag{21}$$

where $S_1 \cap S_2 = \emptyset$ and $S_1 \cup S_2 = S$. Then choosing n_1 collocation points on S_1 and n_2 points on $S_2, n_1 + n_2 = n+1$ in $\mathbb{R}^2$ or $n_1 + n_2 = n$

in $\mathbb{R}^3$, $\{a_j\}$ in Eqn. (16) or Eqn. (18) can be obtained by solving

$$\begin{cases} \sum_{j=1}^{n_1} a_j G(\mathbf{P}_k, \mathbf{Q}_j) + \delta_d c = g_1(\mathbf{P}_k), & 1 \le k \le n_1, \\ \sum_{j=n_1+1}^{n_1+n_2} a_j \dfrac{\partial}{\partial n_{\mathbf{P}}} G(\mathbf{P}_k, \mathbf{Q}_j) = g_2(\mathbf{P}_k), & n_1+1 \le k \le n_1+n_2, \end{cases} \tag{22}$$

where

$$\delta_d = \begin{cases} 1, & \text{for } d = 2, \\ 0, & \text{for } d = 3. \end{cases}$$

Further, the MFS can accommodate nontraditional boundary conditions as easily as the more traditional Dirichlet or mixed boundary conditions. An interesting class of such conditions are the *oblique* boundary conditions

$$a(\mathbf{P}) + b(\mathbf{P}) \frac{\partial u}{\partial \tau} = g(\mathbf{P}), \quad \mathbf{P} \in S, \tag{23}$$

where τ is a unit vector field on S [30]. When $a = 0, \tau = n$, the unit normal, we have *Neumann* conditions and when $a \neq 0, b \neq 0, \tau = n$ we have *Robin* conditions. In a number of important problems in geodesy $\tau \neq n$ and then using Eqn. (3) or Eqn. (5) leads to Cauchy singular or hypersingular integral equations which can be difficult to solve numerically [30]. However, the MFS can be implemented as in Eqn. (22). In principle, no additional problems should occur. This problem was discussed in [31] where some completeness results were given, but no numerical results were obtained. In view of the importance of this class of problems, we feel that this area should be a fruitful one for research.

2.2 Implementation

Although the MFS is usually straightforward to set up and program [2], there are many practical and theoretical questions which need to be considered. Of these, two of the most critical are the choice of source points $\{\mathbf{Q}_j\}$ and collocation points $\{\mathbf{P}_k\}$. This has been a source of much controversy and until recently there has been little theoretical guidance [2]. We consider the choice of source points first.

Generally, there have been two approaches to choosing $\{\mathbf{Q}_j\}$ - fixed and adaptive. In a fixed method $\{\mathbf{Q}_j\}$ are chosen a priori in

some fashion. In our work we have relied on the approximation results of Bogomolny [22] and the convergence result of Cheng [19] when S and $\hat{S}$ are both circles. In both of these works it is shown that the accuracy of the approximation improves as $\hat{S}$ is moved farther away from S. Cheng [19] and Kutsrada and Okamoto [17] show that for analytic data g in Eqn. (2) the error $\|u - u_n\|_\infty \leq c\,(r/R)^n$, where r is the radius of S and R is the radius of $\hat{S}$. Theoretically, in this case $R = \infty$ is the optimal choice. Recent work by Katurada (discussed in Section 2.4) indicates that this result is also true for arbitrary analytic curves S in $\mathbb{R}^2$ [18]. As a consequence, we have usually chosen $\hat{S}$ to be a circle of large radius R in $\mathbb{R}^2$ and a sphere of large radius R in $\mathbb{R}^3$. The source points are then chosen equally spaced around $\hat{S}$ in $\mathbb{R}^2$ and equally spaced in the polar coordinates (ϕ, θ) in $\mathbb{R}^3$ [11]. Because the MFS equations can become highly ill-conditioned as R increases [2, 20, 21], we have generally limited R to be about five times the diameter of D. Despite the ill-conditioning, the accuracy of the numerical solution is largely unaffected [2, 11, 22] - a curious feature of the method which has puzzled many researchers. Some light is shed on this by Kitigawa [20, 21] and will be discussed further in Section 2.4. It is interesting to note that this behavior is shared by other boundary methods based on integral equations of the first kind. Recent work by Christiansen and Saranen [32] and Christiansen and Hansen [33] suggests that for this class of problems the usual condition number is not an appropriate measure of numerical stability. An unintended consequence of this behavior (encountered by us and others) is that if one uses standard linear solvers, then one may find that the routine will abort with an error message indicating that the system is singular. The reason for this appears to be that algorithms based on Gaussian elimination are monitored by a condition number estimator - which we believe is inappropriate for this class of problems. So far, our remedy has been to use our own solver (a standard one, based on Gaussian elimination with partial pivoting), without any check on the condition number. This has generally worked without difficulty. Although we have only anecdotal evidence, it is possible that researchers may have been 'scared away' on encountering this problem.

In adaptive methods the coefficients in Eqn. (16) and Eqn. (18) are chosen by least squares with the source points as parameters to be determined along with the coefficients $\{a_j\}$. In the method developed

by Fairweather and Kargeorghis [7-9] n unknown source points $\{\mathbf{Q}_j\}$ are chosen and m fixed collocation points (usually $m \geq n$) are chosen on S. One then considers the error measure ($\{\mathbf{Q}_j\}$ is the set of source points)

$$\epsilon_n = \sum_{k=1}^{m} \left[u_n\left(\mathbf{P}_k, \{\mathbf{Q}_j\}\right) - g(\mathbf{P}_k)\right]^2 \tag{24}$$

which is minimized simultaneously with respected to $\{a_j\}$ and $\{\mathbf{P}_k\}$. This is a nonlinear optimization problem which can be quite time consuming to solve [7-9]. To the best of our knowledge no detailed comparison has been made between the fixed and adaptive methods of choosing $\{\mathbf{Q}_j\}$. In this regard, a curious feature of the adaptive method is that the optimal solution often yields source points close to S, which seems to contradict the theoretical results in [15, 17-18, 19, 22].

As a compromise between these two approaches, one may choose the source points to be fixed on a circle or sphere of large radius R and then minimize ϵ_n in (24) to determine the coefficients of u_n. This was the approach taken by Bogomolny [22] and there is some numerical indication that this approach may be the most efficient [34]. To avoid choosing R, a priori, one could allow R to be unknown as well.

If the boundary of S in $\mathbb{R}^2$ is parametrized by

$$(x(s), y(s)), \quad 0 \leq s \leq L, \tag{25}$$

then we have generally chosen the collocation points to be of the form

$$\mathbf{P}_k = \left(x\left(\frac{kL}{n+1}\right), y\left(\frac{kL}{n+1}\right)\right), \quad 1 \leq k \leq n+1. \tag{26}$$

In $\mathbb{R}^3$, if S is parametrized by

$$(x(s,t), y(s,t), z(s,t)), \quad 0 \leq s \leq L, \quad 0 \leq t \leq M, \tag{27}$$

then we use

$$\left(x\left(\frac{jL}{p}, \frac{kM}{m}\right), y\left(\frac{jL}{p}, \frac{kM}{m}\right), z\left(\frac{jL}{p}, \frac{kM}{m}\right)\right), \tag{28}$$

$1 \leq j \leq p, 1 \leq k \leq m, n = mp$, as collocation points. Similar choices have been made in the adaptive method [7-9].

Again, this choice has been motivated by Cheng's results where equally spaced source and collocation points were used when S and $\hat{S}$ are circles. However, when S is not a circle this choice may not be optimal. In [18] it is shown that in order to guarantee the convergence of the MFS for Eqn. (1) - Eqn. (2) in $\mathbb{R}^2$ that $\{\mathbf{P}_k\}$ needs to be chosen as

$$\mathbf{P}_k = \Phi^{-1}(\hat{\mathbf{P}}_k) \tag{29}$$

where Φ is a conformal mapping of D onto a disc D_r of radius r and $\left\{\hat{\mathbf{P}}_k\right\}$ are equally spaced about S_r, the boundary of D_r. (In this case $\{\mathbf{Q}_j\}$ are defined by $\mathbf{Q}_j = \Phi^{-1}(\hat{\mathbf{Q}}_j)$ where $\left\{\hat{\mathbf{Q}}_j\right\}$ are equally spaced about a circle of radius $R > r$.) Unfortunately, this leads to an expensive algorithm (unless Φ is known), since one would need to compute Φ. Some modifications of this choice are discussed in Section 2.4.2. They compare favorably with the choice given by Eqn. (29). However, these theoretical results indicate that establishing convergence of the MFS is quite technical and almost everything needs to be done. This contrasts sharply with its ease of implementation.

2.3 Nonsmooth solutions

As we have indicated, when the boundary of S and the boundary data are smooth, the MFS converges rapidly and numerical results corroborate this [2]. In this case the solution of the BVP is smooth and this accounts for the observed convergence behavior. However, in many situations either S or the data are not smooth, and then generally the solution to Eqn. (1) is not smooth as well. In those cases where the solution is smooth, even if S and the data are not, the convergence of the MFS seems to behave as in the smooth case [2]. When this is not the case, the MFS may exhibit slow convergence, even if it converges at all. To deal with this complication, the MFS needs to be modified in some fashion as in the BEM [35] or FEM [27].

In the BEM the two most common approaches to this problem are to use *graded meshes* in the neighborhood of singular points [2, 36] and/or to subtract off known singular solutions [35]. Both of these methods require knowing the explicit analytic behavior of u in the neighborhood of the singularities [2, 36]. For Laplace's equation this behavior has been extensively investigated, both in $\mathbb{R}^2$ and $\mathbb{R}^3$ [37], but numerical implementations have generally only been given in $\mathbb{R}^2$.

As shown by Fairweather and Karageorghis [9], Karageorghis [38] and Poullikkas, Karageorghis and Georgiou [39], these methods can be used with the MFS as well. Here we briefly discuss some results given in [38, 39].

For simplicity, suppose that D is now a polygon with vertices $(v_1, v_2, \cdots, v_p)$. In general, solutions to Laplace's equation will be singular at the vertices and/or points where the boundary conditions change type (such as Dirichlet to Neumann) [2, 38, 39]. In the interior, the solution will generally be at least C^2. Suppose the solution is singular in the neighborhood of v_1, then introducing a local polar coordinate system (r, θ) with origin at v_1, the solution will be of the form [38, 39]

$$u(r,\theta) = \sum_{k=1}^{\infty} \alpha_k r^{\lambda_k} f_k(\theta) \tag{30}$$

where $\{\lambda_k, f_k(\theta)\}$ are known and depend on the angle at v_1 ($r^{\lambda_k} f_k(\theta)$ are harmonic) and the nature of the boundary data [27]. Usually $|\lambda_1| < 1$ and $\lambda_1 < \lambda_2 < \cdots < \lambda_k < \cdots$. Using Eqn. (30) we define a modified MFS approximation

$$u_n(\mathbf{P}) = \sum_{j=1}^{n} a_j G(\mathbf{P}, \mathbf{Q}_j) + \sum_{j=1}^{k} \alpha_j r^{\lambda_j} f_j(\theta) + c \tag{31}$$

where the coefficients $\{\{a_j\}, \{\alpha_j\}, c\}$ can be determined by collocation or least squares. As an example we discuss some results given by Karageorghis [38].

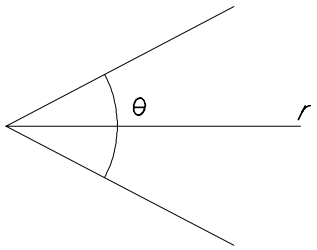

Figure 2. Local polar coordinates.

Example 2.3.1 (The Motz problem) A standard example for testing algorithms for solving singular BVPs is the Motz problem (see Fig.

3). Here we solve $\Delta u = 0$ in the rectangle ABCD with boundary conditions

$$\frac{\partial u(\mathbf{P})}{\partial n_{\mathbf{P}}} = 0, \quad \mathbf{P} \in OA, BC, CD, \tag{32}$$

$$u = 1000, \quad \mathbf{P} \in AB, \tag{33}$$

$$u = 500, \quad \mathbf{P} \in DO. \tag{34}$$

It is known that u has a boundary singularity at the point O of the form [38, 39]

$$u(r,\theta) = 500 + \sum_{j=1}^{\infty} \alpha_j r^{\frac{2j-1}{2}} \cos\left(\frac{2j-1}{2}\theta\right). \tag{35}$$

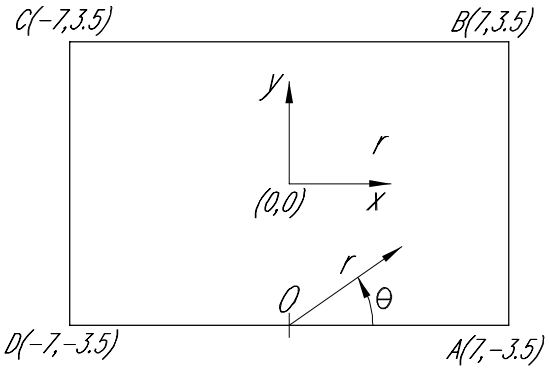

Figure 3. The Motz problem.

To approximate u the approximation in Eqn. (31) was used in [38] with $k = 2$ and $c = 0$ and the coefficients were determined by adaptive least squares. For comparison purposes the problem was also solved using the standard MFS with $\alpha_1 = \alpha_2 = 0$. In Table 1 we give values of u_n at O for various values of n and collocation points m.

The improvement in using Eqn. (31) rather than Eqn. (30) is obvious. The improvement in accuracy at other points is comparable [38].

Table 1. Approximate solution of the Motz Problem at O.

n	m	MFS value	Modified MFS
8	72	589	-
10	96	571	-
12	120	570	-
5	48	-	506
8	72	-	500
10	96	-	500

To overcome the necessity of determining the singular functions $\left\{r^{\lambda_k} f_k(\theta)\right\}$ in (31), Poullikkas *et al* [39] proposed the following modification. Rather than use the known singular function, they suggested using a singular function of the form

$$u_s(r,\theta) = \alpha r^{\beta} \cos(\beta\theta) \tag{36}$$

where (α, β) are assumed unknown and determined by least squares as before. For comparison purposes they considered four algorithms: (i) MFS (ii) modified MFS, α unknown, β known (iii) modified MFS; (α, β) unknown (iv) modified MFS using Eqn. (31) with $k = 2$. The values of u_n at O are shown in Table 2.

Table 2. Comparison of MFS and modified MFS

$n = 7, m = 66$			
MFS	MFS	MFS	MFS
	α unknown	(α, β) unknown	(α_1, α_2) unknown
618.48	503.96	496.80	500.26
Exact value: 500			

Again we see that the modified MFS using Eqn. (36) improves over the MFS but not as much as when the exact analytic form of the singular term is known.

Last we note, by using a superposition approach as in [40], we can accommodate multiple singularities in u.

2.4 Convergence and stability of the MFS

2.4.1 Convergence

Although the MFS has been used for over 30 years [2, 41], the theoretical basis of this method is of recent origin [17-19]. In Cheng's

thesis [19] he proves convergence of the MFS for Laplace's equation in $\mathbb{R}^2$ where S and $\hat{S}$ in Eqn. (18) - Eqn. (19) are circles of radius ρ and R respectively and the source and collocation points are uniformly distributed on S and $\hat{S}$. A similar result was given by Katsurada and Okamoto [17] who weakened the analyticity requirements on g used by Cheng. In further work, Katsurada [18] and Katsurada and Okamoto [42] extended these results to the case where D is a simply connected bounded region in $\mathbb{R}^2$ with an analytic boundary S. Here, we state a number of their results and briefly indicate the method of proof. Since the results are quite technical, we will omit many of the details. Full proofs can be found in [18]. We begin with a statement of their convergence theorem [17] when S and $\hat{S}$ are circles. For convenience in notation we consider $\mathbb{R}^2$ to be the complex numbers $\mathbb{C}$ so that if $z = x + iy \in \mathbb{C}$, $|z| = \|(x, y)\|$.

Theorem 1 *Let $D\rho$ be the disc of radius $\rho; D\rho = \{|z| < \rho\}$ with boundary $S\rho = \{|z| = \rho\}$. Similarly, let $\hat{S}_R = \{|z| = R\}, R > \rho$ and let*

$$\mathbf{Q}_j = R\omega^{j-1}, \quad \mathbf{P}_k = \rho\omega^{k-1}, \quad 1 \leq k \leq n, \tag{37}$$

where $(i^2 = -1)$ and

$$\omega = \exp(2\pi i/n). \tag{38}$$

Let $u_n(\mathbf{P})$ be the MFS collocation approximation to u in Eqn. (1) - Eqn. (2). Then for all n sufficiently large u_n exists, is unique and converges uniformly to u in $D\rho \cup S\rho$. Moreover, if u can be extended to a harmonic function in $\mathbb{C}$, then we have the error bound

$$\|u - u_n\|_\infty \leq c\lambda^n \tag{39}$$

where $\lambda \leq \rho/R < 1$ and c is independent of n (but generally depends on u).

As pointed out previously, this theorem establishes the spectral convergence of the MFS in this special case and confirms the observation that its convergence improves as R increases.

If the constant in Eqn. (19) is omitted, then one has to impose the additional conditions, $R \neq 1$ and $R^n - \rho^n \neq 1$ [17, 18]. The proofs in [18, 19] depend on a detailed, explicit analysis of the Fourier series of u and u_n.

For application of this result to Poisson's equation it is important to know how c in Eqn. (39) depends on the solution u. For this we have the bound [18]

$$\|u - u_n\|_{s(r)} \leq cn^p (r/r_0)^{n/2} \|u\|_{t(r_0)} \tag{40}$$

where $r_0 > \rho$, r satisfies, $r \neq (r_0, R)$ and

$$\max\left\{\rho^2 r_0, r_0(\rho/R)^2\right\} \leq r \leq \min\left\{R^2/r_0, r_0\right\}, \quad r \neq (r_0, R), \tag{41}$$

and p depends on $(s, t, r/\rho, r_0/\rho)$ and is independent of n.

Here, $\|\cdot\|_{s(r)}$ denotes the 's'th Sobolev norm of periodic functions on S_r and $\|\cdot\|_{t(r_0)}$ is the 't'th Sobolev norm of functions on S_{r_0}. Now, if $s > 1/2$, it follows by Sobolev's inequality [2, 27] that

$$\|u\|_{\infty, S_r} \leq c \|u\|_{s(r)} \tag{42}$$

where $\|\cdot\|_{\infty, S_r}$ is the maximum norm on S_r. Since u and u_n are harmonic in S_r we have by the maximum principle, that

$$\|u - u_n\|_{\infty, D_r} \leq \|u - u_n\|_{\infty, S_r}. \tag{43}$$

Now choosing $r > \rho$ and using

$$\|u - u_n\|_{\infty, D\rho} \leq \|u - u_n\|_{\infty, D_r} \tag{44}$$

gives

$$\begin{aligned} \|u - u_n\|_{\infty, D\rho} &\leq \|u - u_n\|_{\infty, S_r} \\ &\leq c \|u - u_n\|_{S(r)} \leq cn^p (r/r_0)^{n/2} \|u\|_{t(r_0)}. \end{aligned} \tag{45}$$

In [17] somewhat sharper bounds were given for $\|u - u_n\|_\infty$. There it was shown that

$$\|u - u_n\|_\infty \leq c(\rho/r_0)^{n/2} \|u\|_{\infty, r_0}, r_0 < R^2/\rho, \tag{46}$$

$$\|u - u_n\|_\infty \leq cn(\rho/R)^n \|u\|_{\infty, r_0}, r_0 = R^2/\rho, \tag{47}$$

$$\|u - u_n\|_\infty \leq c(\rho/R)^n \|u\|_{\infty, r_0}, r_0 > R^2/\rho, \tag{48}$$

where $\|\cdot\|_{\infty, r_0}$ is the uniform norm on $\{\|z\| = r_0\}$.

In [18] Katsurada extended Theorem 1 to the case where S is an analytic Jordan curve boundary D. To do this, let Φ be a conformal

mapping of $D \cup S$ onto the unit disk $D_1 = \{|z| \leq 1\}$ (such a mapping exists by the Riemann mapping theorem [43]) and define

$$\mathbf{Q}_j = \Phi^{-1}(R\omega^{j-1}) \text{ and } \mathbf{P}_j = \Phi^{-1}(\omega^{j-1}), \quad 1 \leq j \leq n, \tag{49}$$

where Φ^{-1} is the inverse of Φ and $R > 1$. Then using $\{\mathbf{Q}_j\}_1^n$ as source points and $\{\mathbf{P}_j\}_1^n$ as collocation points (Note: $\mathbf{P}_j \in S$), and defining the MFS approximation u_n by Eqn. (19) with $c = 0$, we have the following theorem.

Theorem 2 *Under the conditions stated previously, and assuming that g in (2) is analytic, u_n exists for all n sufficiently large, is unique and there exist constants $c, 0 \leq \lambda < 1$, and $n_0, n \geq n_0$ such that*

$$\|u - u_n\|_\infty \leq c\lambda^n, \quad n \geq n_0. \tag{50}$$

In general, λ decreases as R increases (specific conditions may be found [18]) and estimates analogous to (40) in Sobolev spaces of analytic functions are given in [18]. Katsurada modified this procedure to consider exterior, rather than interior conformal mappings [44].

As we have already pointed out, the proofs of Eqn. (39) and Eqn. (50) are quite technical, but the basic idea is to use an argument relating to the fact that the MFS approximation u_n may be regarded as a discretization of the single layer integral equation (8). The convergence proofs then proceed along the lines of Arnold-Wendland [45] and Cheng [19] for the classical single layer equation.

To be more specific, letting $\Psi = \Phi^{-1}$, taking $\rho = 1$ for convenience and defining ("$\circ$" denotes composition)

$$\tilde{u} = u \circ \Psi, \quad \tilde{g} = g \circ \Psi, \quad \tilde{u}_n = u_n \circ \Psi, \tag{51}$$

then $\tilde{u} = \tilde{g}$ on D, and

$$\tilde{u}_n\left(\omega^{j-1}\right) = \tilde{g}\left(\omega^{j-1}\right), \quad 1 \leq j \leq n. \tag{52}$$

Since Φ is conformal, $\Delta\tilde{u} = 0$ and $\Delta\tilde{u}_n = 0$ in D_1.

Now define

$$k(\mathbf{P}, \mathbf{Q}) = \frac{1}{2\pi} \log |\Psi(\mathbf{P}) - \Psi(\mathbf{Q})|, \quad \mathbf{Q} \in S_1, \quad \mathbf{P} \in S_R. \tag{53}$$

Since,

$$\tilde{u}_n(\mathbf{P}) = u_n(\Psi(\mathbf{P})) = \frac{1}{2\pi}\sum_{j=1}^{n} a_j \log|\Psi(\mathbf{P}) - \Psi(\mathbf{Q}_j)| \tag{54}$$

$$= \frac{1}{2\pi}\sum_{j=1}^{n} a_j \log\left|\Psi(\mathbf{P}) - R\omega^{j-1}\right| = \sum_{j=1}^{n} a_j k(\mathbf{P}, R\omega^{j-1}) \tag{55}$$

The function $\tilde{u}_n$ may be considered as an approximation to the boundary value problem

$$\Delta\tilde{u}(\mathbf{P}) = 0, \quad \mathbf{P} \in D_1, \tag{56}$$

$$\tilde{u}(\mathbf{P}) = \tilde{g}, \quad \mathbf{P} \in S_1. \tag{57}$$

Now suppose that there is a solution $\tilde{\sigma}$ to the single layer equation

$$\int_{S_R} k(\mathbf{P}, \mathbf{Q})\tilde{\sigma}(\mathbf{Q})\, ds = \tilde{g}, \quad \mathbf{P} \in S_R, \tag{58}$$

then

$$\tilde{u}(\mathbf{P}) = \int_{S_R} k(\mathbf{P}, \mathbf{Q})\tilde{\sigma}(\mathbf{Q})\, ds, \quad \mathbf{P} \in D_1 \tag{59}$$

is a solution to Eqn. (56) - Eqn. (57). We will now show that the MFS may be viewed as a discretization of (59) by an approximate collocation method. Before doing this, we note that Eqn. (59) can be written equivalently in the form

$$-R\int_0^1 k(e^{2\pi i t}, R\, e^{2\pi i \tau})\sigma(\tau)\, d\tau = g(t), \quad 0 \le t \le 1, \tag{60}$$

where

$$g(t) \equiv \tilde{g}(e^{2\pi i t}) \text{ and } \sigma(t) = \tilde{\sigma}(Re^{2\pi i t}). \tag{61}$$

In operator form, Eqn. (59) and Eqn. (60) become

$$A\sigma = g \text{ and } \tilde{A}\tilde{\sigma} = \tilde{g}. \tag{62}$$

In analogy to the method of Arnold-Wendland [45] for the case $R = 1$ (standard BEM), we look for approximations to σ of the form

$$\sigma_n(t) = \sum_{j=1}^{n} a_j \delta(t - \frac{j}{n}), \tag{63}$$

where $\delta(\cdot)$ is the Dirac delta function. Substituting σ_n into Eqn. (60) and collocating at the points $\{k/n\}_1^n$ gives the equations

$$-R\sum_{j=1}^{n} a_j\, k(e^{2\pi ik/n}, Re^{2\pi ij/n}) = g(\frac{k}{n}), \quad 1 \le k \le n, \tag{64}$$

for $\{a_j\}_1^n$. The *modified MFS approximation* $\tilde{u}_n$ is then given by

$$\tilde{u}_n(\mathbf{P}) = A\sigma_n \tag{65}$$

and via Eqn. (51) is equivalent to the MFS approximation u_n. Hence, to analyze the convergence of u_n it suffices to analyze the convergence of $\tilde{u}_n$ and thus the convergence of σ_n. This is the approach followed in [18].

To do this one must consider the mapping properties of the operator A in Eqn. (60) on the Hilbert space $\mathcal{H}_{s,\varepsilon}$, $\varepsilon > 0, s \in \mathbb{R}$ where

$$\mathcal{H}_{s,\varepsilon} = \left\{ u : u \text{ is a periodic distribution on [0,1] and } \|u\|_{s,\varepsilon} < \infty \right\},$$

where

$$\|u\|_{s,\varepsilon} = \left[\sum_{n=-\infty}^{\infty} |\hat{u}(n)|^2\, \varepsilon^{2|n|} \bar{n}^{2s} \right]^{1/2} \tag{66}$$

and

$$\hat{u}(n) = \int_0^1 u(t) e^{-2\pi int} dt, \quad \bar{n} = \max(2\pi, |n|) \tag{67}$$

(Note: for $\varepsilon = 1, \mathcal{H}_{s,1} \equiv H_s, s \in \mathbb{R}$, are the usual Sobolev spaces of periodic distributions on $[0,1]$ [2, 27].) This is done by decomposing the operator A as

$$A = H + K \tag{68}$$

where

$$H\sigma(t) = -R \int_0^1 \log \left| e^{2\pi it} - Re^{2\pi i\tau} \right| \sigma(\tau) d\tau \tag{69}$$

(this is the operator for the circle - circle case) and

$$H\sigma(t) = (A - H)\sigma(t) = -R \int_0^1 \log \left| \frac{\Psi(e^{2\pi it}) - \Psi(Re^{2\pi i\tau})}{e^{2\pi it} - Re^{2\pi i\tau}} \right| \sigma(\tau) d\tau. \tag{70}$$

Then it can be shown by direct analysis of the Fourier coefficients $\widehat{H\sigma}(n) = \hat{G}(n)\hat{\sigma}(n)$,

$$\hat{G}(n) = \begin{cases} \dfrac{R}{2\pi\,|n|}\left(\dfrac{1}{R}\right)^{|n|}, & n \neq 0, \\ -R\log R, & n = 0, \end{cases} \tag{71}$$

that $H : \mathcal{H}_{s,\varepsilon} \to \mathcal{H}_{s+1,\varepsilon R}$ is bounded and if $R \neq 1$, H is an isomorphism. With some further restrictions on ε (depending on Ψ) $K : \mathcal{H}_{s,\varepsilon} \to \mathcal{H}_{s+1,\varepsilon R}$ is compact [18]. (Again, this is done by a direct analysis of the Fourier coefficients of the kernel of K.) It then follows that if the capacity of $S \neq 1$, then $A : \mathcal{H}_{s,\varepsilon} \to \mathcal{H}_{s,\varepsilon R}$ is an isomorphism [18]. Using these properties, the convergence of σ_n can be reduced to the convergence σ_n in the circle case. In the latter case that is again established by a detailed Fourier analysis which is given in the Appendix of [18] where it is shown that

$$\|\sigma - \sigma_n\|_{s,\varepsilon} \leq c\lambda^n \|\sigma\|_{t,\delta}\,, 0 \leq \lambda < 1. \tag{72}$$

(t, δ are given in [18]). Then using the facts that H and A are isomorphisms ($\hat{\varepsilon} = \varepsilon R$) [18],

$$\begin{aligned} \|\sigma - \sigma_n\|_{s,\varepsilon} &\leq \left\|AA^{-1}(\sigma - \sigma_n)\right\|_{s,\varepsilon} \leq \left\|A^{-1}\right\| \|A(\sigma - \sigma_n)\|_{s,\hat{\varepsilon}} \\ &\leq c\,\|A(\sigma - \sigma_n)\|_{s+1,\hat{\varepsilon}} \leq c\left\|HH^{-1}A(\sigma - \sigma_n)\right\|_{s+1,\hat{\varepsilon}} \\ &\leq c\left\|H^{-1}A(\sigma - \sigma_n)\right\|_{s,\varepsilon}. \end{aligned} \tag{73}$$

Defining,

$$w_n = \sigma_n, \tag{74}$$

and

$$w = \sigma_n - H^{-1}A(\sigma - \sigma_n)\,, \tag{75}$$

one easily shows that $H^{-1}A(\sigma - \sigma_n) = w_n - w$ and $Hw_n = Hw = g$ on Λ_n ($\Lambda_n = \{k/n\}_1^n$). Then using Eqn. (72) and Eqn. (73) with $\sigma_n = w_n$

$$\|\sigma - \sigma_n\|_{s,\varepsilon} \leq c\,\|w - w_n\|_{s,\varepsilon} \leq c\lambda^n \|w\|_{t,\delta}\,. \tag{76}$$

Since $w = \sigma_n + H^{-1}(H - A)(\sigma - \sigma_n)$,

$$\begin{aligned} \|w\|_{t,\delta} &= \left\|\sigma + H^{-1}(H - A)(\sigma - \sigma_n)\right\|_{t,\delta} \\ &\leq \|\sigma\|_{t,\delta} + \left\|H^{-1}(H - A)(\sigma - \sigma_n)\right\|_{t,\delta} \end{aligned}$$

$$
\begin{aligned}
&\leq \|\sigma\|_{t,\delta} + c\,\|(H-A)(\sigma-\sigma_n)\|_{t,\delta} \\
&\leq \|\sigma\|_{t,\delta} + c\,\|(H-A)(\sigma-\sigma_n)\|_{t+1,R\delta} \\
&\leq \|\sigma\|_{t,\delta} + c\,\|\sigma-\sigma_n\|_{s,\varepsilon}\,. \qquad (77)
\end{aligned}
$$

since $H - A = -K : \mathcal{H}_{s,\varepsilon} \to \mathcal{H}_{t+1,R\delta}$ is bounded [18]. Thus,

$$
\|\sigma-\sigma_n\|_{s,\varepsilon} \leq c\lambda^n \left(\|\sigma\|_{t,\delta} + c\,\|\sigma-\sigma_n\|_{s,\varepsilon} \right), \qquad (78)
$$

so that for sufficiently large n

$$
\|\sigma-\sigma_n\|_{s,\varepsilon} \leq c\lambda^n \|\sigma\|_{t,\delta}\,. \qquad (79)
$$

From Eqn. (79) and the boundedness of A it follows that $A\sigma_n$ converges to $A\sigma$. Convergence of $\tilde{u}_n$ (hence of u_n) now follows from the maximum principle and Sobolev's inequality for n sufficiently large.

2.4.2 Source and collocation points in $\mathbb{R}^2$

As already indicated, we have had considerable success in using the MFS by choosing the source points uniformly distributed on circle of large radius R and the collocation points uniformly distributed in angle on S. According to Theorem 1 this choice guarantees exponential convergence of u_n when S is a circle and g in Eqn. (2) is analytic. However, for other cases, we have no guarantee of convergence for this choice - although convergence has generally been observed numerically [2, 10-12]. For mathematical consistency, it is desirable to use algorithms whose theoretical properties are understood. For this reason it is of interest to implement the choice given in Eqn. (49). However, to do this one needs to compute the conformal mapping Ψ. Katsurada and Okamoto provided an efficient algorithm for doing this [42] . We briefly describe their procedure.

The mapping Ψ can be viewed as a complexification of a parametrization $(x(\theta), y(\theta))$ of S given by

$$
f(\theta) = x(\theta) + iy(\theta) = \sum_{n=-\infty}^{\infty} \beta_n e^{in\theta}, \quad 0 \leq \theta \leq 2\pi. \qquad (80)
$$

Then, since S is assumed to be analytic, f can be extended analytically to a strip $b < |z| < 1/b$ about S_1 by

$$
f(z) = \sum_{n=-\infty}^{\infty} \beta_n z^n. \qquad (81)
$$

To determine $\{\beta_n\}$ Katsurada and Okamoto proposed the following:

(i) Choose n points $\{\mathbf{Q}_j = x_j + iy_j\}_1^n$ on S.

(ii) Compute $\{\beta_k\}_{-n/2+1}^{n/2+1}$ by solving

$$f(w^{k-1}) = \mathbf{x}_k, \quad \mathbf{x}_k = \Psi(R, \omega^{k-1}), \quad b < R < 1/b, \quad 1 \le k \le n. \tag{82}$$

The source points are then given by

$$\mathbf{P}_j = \sum_{k=-n/2+1}^{n/2+1} \hat{\beta}_k \left(R\omega^{j-1}\right), \quad 1 \le j \le n, \tag{83}$$

where $\hat{\beta}_n$ are the approximations to β_n given by (i)-(ii) and $1 < R < 1/k$. In [42] it is shown that $\left\{\hat{\beta}_n\right\}$ can be computed in $O(n \log n)$ operations using the Fast Fourier Transform (FFT). However, because the accuracy of $\left\{\hat{\beta}_n\right\}$ is poor [42], they suggested the following modification. Let $\mathbf{Q}_{k-1/2}$ be a point on the arc between $\mathbf{Q}_{k-1}$ and $\mathbf{Q}_k, 1 \le k \le n$, and assume that $f(w^{k-1-1/2}) = \mathbf{Q}_{k-1/2}$. Then compute

$$c_j = \sum_{k=1}^{n} \mathbf{Q}_k \omega^{-(k-1)(j-1)} \tag{84}$$

and

$$d_j = \sum_{k=1}^{n} \mathbf{Q}_{k-1/2} \omega^{-(k-1)(j-1)} \tag{85}$$

($\{c_j\}$ and $\{d_j\}$ can be computed by FFT [42]) and define

$$\widehat{\widehat{\beta}}_{j-1} = \frac{c_j + \omega^{(j-1)/2} d_j}{2n}, \quad 1 \le j \le n/2 + 1, \tag{86}$$

and

$$\widehat{\widehat{\beta}}_{j-1-n} = \frac{c_j + \omega^{(j-1)/2} d_j}{2n}, \quad n/2 + 1 \le j \le n, \tag{87}$$

then the source points are given by Eqn. (83) using $\left\{\widehat{\widehat{\beta}}_j\right\}$ rather than $\left\{\hat{\beta}_j\right\}$. Again, $\left\{\widehat{\widehat{\beta}}_j\right\}$ can be computed in $O(n \log n)$ operations using

FFT. This is generally a fraction of the $O(n^3)$ operations required to compute u_n.

To test this procedure the authors solved Eqn. (1) - Eqn. (2) with S, the Oval of Casini, as in Example 4.1.1 of this chapter using $g = \mathrm{Re}(z^n), 1 \leq n \leq 6$, as boundary values. In this case the interior conformal mapping $\Phi : D \to D_1$ and the exterior one $\tilde{\Phi} : D \to \bar{D}_1$ are known analytically [42]. Using this they considered five MFS algorithms for solving Eqn. (1) - Eqn. (2):

(i) the MFS with source and collocation points given in Eqn. (49);

(ii) the MFS with source and collocation points determined by the exterior conformal mapping Φ [44];

(iii) the MFS with source points given by Eqn. (84) - Eqn. (87) and collocation points equally spaced in arc length on S;

(iv) the MFS with source points equally spaced on a circle of radius R and collocation points $\mathbf{P}_k = \rho_k \omega^{k-1}$ where ρ_k is chosen so that $\mathbf{P}_k \in S$. (This circle rule is similar to our algorithm.)

(v) the MFS with $\{\mathbf{P}_k\}$ chosen as in (iv) and $\mathbf{Q}_j = R\mathbf{P}_j$ (similarity transform). (R was chosen in the range $1 < R \leq 1.5$.)

In all cases, the numerical results, using $n < 100$, showed an exponential decrease in the error with the accuracy improving as R increased [42]. The results using the naive circle rule (iv) were comparable to those using (i)-(iii). However, the circle rule gave a collocation matrix which was more ill-conditioned (as estimated by LINPACK [46]) than the rule (iii) and on the basis of this the authors aborted the calculations using the circle rule for $n = 50$. As we observed earlier, this may not have been necessary as the ill-conditioning may not have been numerically significant. Using (iii) they solved all problems with errors $O(10^{-8})$ for $n \simeq 100$. Again, this is consistent with our own results and may be improved by choosing $R > 1.5$ [42].

Last, we comment that it would be of great interest to extend these results to problems in $\mathbb{R}^3$.

2.5 Stability

As our discussion in Section 2.2 indicates, the ill-conditioning of the MFS equations has been a source of difficulty with this method since

its inception and may have resulted in practioners shying away from the method despite its elegance and efficiency. As we and others have observed [2, 10-12, 22], the ill-conditioning may have little effect on the numerical accuracy of the MFS. Traditionally, in numerical analysis, the amplification of data errors (say, round-off errors) in the numerical solution of n linear equations

$$A\mathbf{x} = \mathbf{b}, \quad \mathbf{x} \in \mathbb{R}^n \text{ or } \mathbf{x} \in \mathbb{C}^n, \tag{88}$$

has been measured by the condition number $k(A)$ of A given by

$$k(A) = \|A\| \left\|A^{-1}\right\|, \tag{89}$$

where $\|\cdot\|$ is a matrix norm. If the spectral norm is used in $\mathbb{R}^n$ or $\mathbb{C}^n$, then

$$k(A) = \sigma_1/\sigma_n \tag{90}$$

where $\sigma_1 \geq \sigma_2 \geq \cdots \geq \sigma_n$ are the *singular values* of A. Typically, ill-conditioning is indicated by very small values of σ_n. However, the usual error bound

$$\frac{\|\mathbf{x} - \hat{\mathbf{x}}\|}{\|\mathbf{x}\|} \leq k(A) \frac{\|\Delta\mathbf{b}\|}{\|\mathbf{b}\|} \tag{91}$$

for

$$(A + \Delta A)\,\mathbf{x} = \mathbf{b} + \Delta\mathbf{b} \tag{92}$$

is often pessimistic and using only $k(A)$ to monitor stability may result in an overly pessimistic view of a given numerical method. In [47] it is shown that a full understanding of the numerical stability of $\mathbf{x}$ in Eqn. (88) requires knowledge of the *complete singular value decomposition (SVD) of* A and not just σ_1 and σ_n. Kitigawa showed that this phenomenon occurs when using the MFS [20, 21] . We consider his results when S is a circle in (1)-(2).

As we have shown, the convergence of the MFS is exponential when g is analytic, but unfortunately the condition number $k(A)$ of the system Eqn. (18) satisfies [20]

$$k(A) = O(n(R/\rho)^{n/2}) \tag{93}$$

which shows that $k(A)$ grows exponentially with n. However, this can be misleading since the coefficients $\{a_j\}$ in Eqn. (16) are usually not of independent interest, rather the solution $u_n(\mathbf{P}) = \sum_{j=1}^{n} a_j G(\mathbf{P}, \mathbf{Q}_j)$

is. What is of importance is how data errors are amplified in u_n, not necessarily in $\{a_j\}$.

To describe Kitigawa's results, choose n points on S given by

$$\bar{\mathbf{P}}_k = \bar{\mathbf{x}} e^{ik\theta}, \quad -\pi/n < \theta \leq \pi/n, \quad 1 \leq k \leq n, \tag{94}$$

where $\bar{\mathbf{x}}$ is a fixed point on S. Denote the vector $\left\{\bar{\mathbf{P}}_k\right\}_1^n$ by $\bar{\mathbf{P}}$, then the values of u_n (denoted by $\mathbf{u}_n$) at $\bar{\mathbf{P}}$ are given by

$$\mathbf{u}_n\left(\bar{\mathbf{P}}\right) = \mathbf{G}(\bar{\mathbf{P}})\mathbf{a} \tag{95}$$

where $\mathbf{a} = (a_1, a_2, \cdots, a_n)$ and

$$\mathbf{G}(\mathbf{P}) = [G(\mathbf{P}_k, \mathbf{Q}_j)], \quad 1 \leq j, k \leq n. \tag{96}$$

If we consider only pertubations $\Delta\mathbf{g}$ to the right-hand side of Eqn. (18), then $\mathbf{u}_n$ is perturbed to $\bar{\mathbf{u}}_n = G(\mathbf{P})\bar{\mathbf{a}}$ and the error $\Delta\mathbf{u}_n$ is given by

$$\Delta\mathbf{u}_n = \bar{\mathbf{u}}_n - \mathbf{u}_n = G(\bar{\mathbf{P}})(\mathbf{a} - \hat{\mathbf{a}}). \tag{97}$$

Since $\Delta\mathbf{u}_n$ is harmonic, by the maximum principle it suffices to show that

$$\|\Delta\mathbf{u}_n\|_\infty \leq \sqrt{n} \left\| \sum * \Theta \right\|_F \|\Delta\mathbf{g}\|_\infty, \tag{98}$$

where $\|\cdot\|_F$ is the Frobenius norm of $\sum * \Theta$ [20], in order to bound $\Delta\mathbf{u}_n$. The matrices $\sum$ and Θ are given by

$$\sum = \left[\sum_{ij}\right], \sum_{ij} = \frac{\sigma_i}{\sigma_j}, \quad 1 \leq i, j \leq n, \tag{99}$$

$$\Theta = [d_{ij}], d_{ij} = \langle \mathbf{v}_i, \bar{\mathbf{v}}_j \rangle, \quad 1 \leq i, j \leq n, \tag{100}$$

Here, $\{\sigma_i\}_1^n$ are the singular values of $G(\mathbf{P})$ and $\{\mathbf{v}_i\}_1^n, \{\mathbf{v}_j\}_1^n$ are the corresponding right singular vectors [20]. The asterisk in Eqn. (98) denotes the pointwise *Hadamard product* of $\sum$ and Θ and $\|\cdot\|_\infty$ is the maximum norm of vectors in $\mathbb{R}^n$ or $\mathbb{C}^n$.

To see the practical significance of this result we display $\sum$ and Θ in greater detail. Hence,

$$\sum = \begin{bmatrix} \frac{\bar{\sigma}_1}{\sigma_1} & \frac{\bar{\sigma}_1}{\sigma_2} & \cdots & \frac{\bar{\sigma}_1}{\sigma_n} \\ \frac{\bar{\sigma}_2}{\sigma_1} & \frac{\bar{\sigma}_2}{\sigma_2} & \cdots & \frac{\bar{\sigma}_2}{\sigma_n} \\ \vdots & \vdots & \ddots & \vdots \\ \frac{\bar{\sigma}_n}{\sigma_1} & \frac{\bar{\sigma}_n}{\sigma_2} & \cdots & \frac{\bar{\sigma}_n}{\sigma_n} \end{bmatrix} \tag{101}$$

and

$$\Theta = \begin{bmatrix} \langle \bar{\mathbf{v}}_1, \mathbf{v}_1 \rangle & \langle \bar{\mathbf{v}}_1, \mathbf{v}_2 \rangle & \cdots & \langle \bar{\mathbf{v}}_1, \mathbf{v}_n \rangle \\ \langle \bar{\mathbf{v}}_2, \mathbf{v}_1 \rangle & \langle \bar{\mathbf{v}}_2, \mathbf{v}_2 \rangle & \cdots & \langle \bar{\mathbf{v}}_2, \mathbf{v}_1 \rangle \\ \vdots & \vdots & \ddots & \vdots \\ \langle \bar{\mathbf{v}}_n, \mathbf{v}_1 \rangle & \langle \bar{\mathbf{v}}_n, \mathbf{v}_2 \rangle & \cdots & \langle \bar{\mathbf{v}}_n, \mathbf{v}_n \rangle \end{bmatrix}. \tag{102}$$

The *amplification matrix* $\sum * \Theta = [\alpha_{ij}], 1 \leq i, j \leq n$, is then given by

$$\alpha_{ij} = \left(\frac{\bar{\sigma}_i}{\sigma_j} \right) \langle \bar{\mathbf{v}}_i, \mathbf{v}_j \rangle \tag{103}$$

and

$$\left\| \sum * \Theta \right\|_F = \left[\sum_{i=1}^{n} \sum_{j=1}^{n} (\alpha_{ij})^2 \right]^{1/2}, \tag{104}$$

so that 'large' values of $|\alpha_{ij}|$ are expected to be deleterious to numerical stability. From Eqn. (103) α_{ij} can be small even if $\bar{\sigma}_i/\sigma_j$ is large provided $|\langle \bar{\mathbf{v}}_i, \mathbf{v}_j \rangle|$ is small. In fact, by the Cauchy-Schwarz inequality $|\langle \bar{\mathbf{v}}_i, \mathbf{v}_j \rangle| \leq \|\bar{\mathbf{v}}_i\| \|\mathbf{v}_j\| = 1$ [20]. Thus $|\alpha_{ij}| \leq |\bar{\sigma}_1/\sigma_n|$ and this bound is often pessimistic.

Now if the collocation matrix is ill-conditioned, then σ_n will be small and $\bar{\sigma}_1$ will be large so that the largest elements of $\sum$ come from the upper right corner in Eqn. (101). Now suppose $\bar{\mathbf{P}} = \mathbf{P}$, then $\bar{\mathbf{v}}_i = \mathbf{v}_i$ and $\langle \mathbf{v}_i, \mathbf{v}_j \rangle = 0, i \neq j, \langle \mathbf{v}_i, \mathbf{v}_i \rangle = 1$ since $\{\mathbf{v}_i\}_1^n$ is an orthonormal basis for $\mathbb{R}^n$ or $\mathbb{C}^n$. Thus, Θ is the $n \times n$ identity matrix I_n and $\sum * \Theta = I_n$ as well. Hence, in this case the problem is *well-conditioned* even if $G(\mathbf{P})$ is *not*. For θ small, it follows by perturbation theory that $\sum * \Theta \simeq I_n$ and the problem will be well-conditioned even if the collocation matrix is not. Roughly speaking, if the elements in the upper right corner of Eqn. (102) are $\simeq 1$, then the overall problem will be ill-conditioned. On the other hand, if they are $\simeq 0$, then we can expect a well-conditioned problem. In [20] Kitigawa suggests looking at the determinant of Θ as a guide.

In a later paper Kitigawa improved on these results [21]. By using the fact that $G(\mathbf{P})$ and $G(\bar{\mathbf{P}})$ are *circulant* matrices he showed that $\Theta = I_n$ and

$$\left| \frac{\bar{\sigma}_i}{\sigma_i} \right| \leq 1, \quad 1 \leq i \leq n, \tag{105}$$

so that $\|\sum * \Theta\|_F \leq \sqrt{n}$. Hence,

$$\|\Delta \mathbf{u_n}\| \leq \sqrt{n} \cdot \sqrt{n} \|\Delta g\|_\infty = n \|\Delta g\|_\infty . \tag{106}$$

Hence, overall, the error is magnified by a quantity of $O(n)$ rather than the pessimistic bound given by Eqn. (93). Since the MFS is exponentially convergent, as discussed previously, n is usually small, so the effect of Eqn. (106) can generally be ignored. This has been our experience in practice.

As we stated at the beginning of this section, this confirms that an understanding of the conditioning of the MFS requires examining the SVD of $G(\mathbf{P}(\theta))$. Obviously, this will substantially increase the cost of the algorithm - but the problem certainly merits further research.

For some specific numerical examples we refer the reader to [20].

3 The MFS for the Helmholtz equation

Although most of the published work on the MFS seems to be for Laplace's equation, other PDEs have also been solved by this technique [8, 13]. Of considerable importance in engineering analysis is the *Helmholtz* equation.

$$\Delta u(\mathbf{P}) + \lambda^2 u(\mathbf{P}) = 0 \tag{107}$$

where $\lambda \in \mathbb{R}$. This equation occurs when looking for time-harmonic solutions of the wave equation [2, 13].

As for Laplace's equation one can formulate a number of boundary value problems for Eqn. (107), typically interior and exterior Dirichlet and Neumann problems [2, 23]. Perhaps the most important class of problems are exterior Neumann problems which arise in the scattering of acoustic and electromagnetic waves from solid scatters [2, 23]. Such problems are of the form

$$\Delta u(\mathbf{P}) + \lambda^2 u(\mathbf{P}) = 0, \quad \mathbf{P} \in \bar{D}, \tag{108}$$

$$\frac{\partial u(\mathbf{P})}{\partial n_{\mathbf{P}}} = g(\mathbf{P}), \quad \mathbf{P} \in S, \tag{109}$$

where we assume that D and S are as described in Section 2 and $\bar{D}$ is the complement of D. Under smoothness conditions on S, solutions to Eqn. (108) - Eqn. (109) satisfying the Sommerfeld radiation condition exist and are unique [2, 23].

As for Laplace's equation, Eqn. (108) - Eqn. (109) can be solved by using standard BEMs, but complications arise which do not occur for Laplace's equation. Most importantly, standard formulations

using single layer potentials give rise to boundary integral equations whose solutions fail to be unique for values of λ which are eigenvalues of the interior Dirichlet problem for Eqn. (107). These values of λ are often called *forbidden* or *fictitious* frequencies [2, 23]. Similar problems occur for the Dirichlet problem [23]. A typical method for dealing with this problem is to express the solutions of Eqn. (108) - Eqn. (109) as a linear combination of single and double layer potentials. Unfortunately, the resulting integral equations are hypersingular and as for Laplace's equation can be difficult to solve numerically [48]. As a consequence, a number of researchers have considered the MFS as an alternative method for solving Eqn. (108) - Eqn. (109).

In contrast to interior problems, here one chooses source points $\{\mathbf{Q}_j\}_1^n$ in D and defines an approximation u_n to u by

$$u_n(\mathbf{P}) = \sum_{j=1}^{n} a_j G(\mathbf{P}, \mathbf{Q}_j; \lambda) \tag{110}$$

where $G(\mathbf{P}, \mathbf{Q}_j; \lambda)$, the fundamental solution of Eqn. (107), is given by

$$G(\mathbf{P}, \mathbf{Q}; \lambda) = \begin{cases} \dfrac{-1}{4i} H_0(\lambda r) & (\mathbf{P}, \mathbf{Q}) \in \mathbb{R}^2, \\ \dfrac{\exp(i\lambda r)}{r}, & (\mathbf{P}, \mathbf{Q}) \in \mathbb{R}^3, \end{cases} \tag{111}$$

$r = \|\mathbf{P} - \mathbf{Q}\|$ and $H_0(\lambda r)$ is a Hankel function of order zero.

Although there appear to be no theoretical results concerning the convergence of u_n, arguing in analogy to Laplace's equation, the source points should be placed on a surface $\hat{S}$ far from the physical surface S [13]. Choosing $\hat{S}$ to be a circle in $\mathbb{R}^2$ or a sphere in $\mathbb{R}^3$ seems reasonable. In addition to the usual advantages of the MFS, it has been observed in [13] that the MFS does not suffer the problem of fictitious frequencies. Numerical results demonstrating the efficacy of this method can be found in [13].

4 The MFS for Poisson's equation

During the past 15 years there has been considerable interest in extending standard BEMs to solve inhomogeneous PDEs. Traditionally this has been a difficult problem because integral reformulations of

the linear elliptic PDE

$$\mathcal{L}u = f \tag{112}$$

contain domain integrals of the form

$$\int_D G(\mathbf{P}, \mathbf{Q}) f(\mathbf{Q}) dv \tag{113}$$

where $G(\mathbf{P}, \mathbf{Q})$ is a fundamental solution of $\mathcal{L}$. Since D is arbitrary and $G(\mathbf{P}, \mathbf{Q})$ is usually singular at $\mathbf{P} = \mathbf{Q}$, the accurate numerical evaluation of Eqn. (113) can be difficult and time consuming [1, 2]. As a consequence, much work in the BEM community has been devoted to alleviating this problem [1, 2]. In the engineering literature the three most used alternatives to direct numerical approximation of (113) have been (i) the *Dual Reciprocity Method* (DRM) [1] (ii) the *Multiple Reciprocity Method* (MRM) [1] and (iii) *Method of Particular Solutions* (MPS) [2, 49]. In [50] we showed that the DRM and the MPS are equivalent when $\mathcal{L} = \Delta$ in Eqn. (112) - Poisson's equation. Hence, we focus on the MPS.

The MPS is an extension of the well-known technique for solving ordinary differential equations by subtracting off a particular solution of Eqn. (112). Thus we define

$$v = u - u_p \tag{114}$$

where u_p satisfies $\mathcal{L}u_p = f$ but not necessarily any boundary conditions for u. By linearity,

$$\mathcal{L}v = \mathcal{L}(u - u_p) = \mathcal{L}u - \mathcal{L}u_p = f - f = 0. \tag{115}$$

Thus v satisfies the *homogeneous* equation

$$\mathcal{L}v = 0, \tag{116}$$

with boundary conditions for v determined by those for u and u_p. In particular, for Poisson's equation Eqn. (116) is Laplace's equation which can then be solved by the MFS. If $\hat{v}$ is an approximation to v, then $\hat{u} = \hat{v} + u_p$ is taken as approximation to u. The remaining problem is to determine u_p.

As is well known, u_p given by Eqn. (113) is a particular solution of Eqn. (112). However, this does not improve matters since we have the same problem as before and a number of techniques have been

proposed to deal with this. In the engineering literature perhaps the best known technique is that introduced in the DRM by Brebbia and Nardini in [51]. Here we approximate f by a finite linear combination of basis functions $\{\varphi_j(\mathbf{P})\}_1^N$. Hence,

$$f(\mathbf{P}) \simeq \hat{f}(\mathbf{P}) = \sum_{j=1}^{N} a_j \varphi_j(\mathbf{P}) \tag{117}$$

where $\{a_j\}_1^N$ are determined in some fashion from f - typically (but not necessarily) by collocation [2]. Then,

$$\hat{f}(\mathbf{P}_k) = f(\mathbf{P}_k) = \sum_{j=1}^{N} a_j \varphi_j(\mathbf{P}_k), \quad 1 \leq k \leq N, \tag{118}$$

where $\{\mathbf{P}_k\}_1^N$ are N points in $\mathbb{R}^d$ (in the DRM they are usually chosen in D [2]). Assuming that Eqn. (118) can be solved uniquely for $\{a_j\}_1^N$, the approximate particular solution $\hat{u}_p$ is given by

$$\hat{u}_p(\mathbf{P}) = \sum_{j=1}^{N} a_j \Psi_j(\mathbf{P}) \tag{119}$$

where

$$\mathcal{L}\Psi_j = \varphi_j, \quad 1 \leq j \leq N. \tag{120}$$

For efficiency, it is important to be able to solve Eqn. (120) analytically.

Another approach to calculating particular solutions was given by Atkinson [52] as discussed in Chapter 9. In [52] it was observed that if f could be extended smoothly to a domain $\hat{D}$ containing D, then

$$\hat{u}_p(\mathbf{P}) = \int_{\hat{D}} G(\mathbf{P}, \mathbf{Q}) f(\mathbf{Q}) dv \tag{121}$$

is also a particular solution. By choosing $\hat{D}$ to be an ellipse in $\mathbb{R}^2$ or an ellipsoid in $\mathbb{R}^3$, a change of variable reduces Eqn. (121) to an integral which can be approximated by standard quadrature methods [52]. In our work we have considered both of these methods. We examine the DRM approach first.

4.1 Radial basis function approximations

To use Eqn. (119) - Eqn. (120) to approximate particular solutions by collocation, one must choose the bases carefully to satisfy three conditions:

(i) they should provide good approximation to a large class of f's for small N;

(ii) the collocation equations Eqn. (118) should be uniquely solvable for general choices of $\{\mathbf{P}_k\}_1^N$;

(iii) they should be simple enough so that Eqn. (120) can be solved analytically.

Using one-dimensional interpolation as a guide, one might consider polynomial or trigonometric bases as appropriate choices [2, 53]. Unfortunately, due to a theorem of Haar [2], this choice can lead to serious problems since the unique solvability of Eqn. (118) *cannot* be guaranteed in these cases if we wish to allow arbitrary choices of $\{\mathbf{P}_k\}$. Haar showed that if the basis functions do not depend on $\{\mathbf{P}_k\}$ then there always exists at least one set of collocation points where the matrix

$$A = \left[\varphi_j\left(\mathbf{P}_k\right)\right]_{(j,k)=1}^N \tag{122}$$

is singular. Apparently, without being aware of Haar's theorem, a number of researchers have attempted to use polynomial and trigonometric approximations and encountered the singularity of A in their work [53].

In the original work on the DRM [51], Brebbia and Nardini made the *ad-hoc* choice

$$\varphi_j\left(\mathbf{P}\right) = 1 + \left\|\mathbf{P} - \mathbf{P}_j\right\| = 1 + r_j \tag{123}$$

where $\|\cdot\|$ is the Euclidean norm in $\mathbb{R}^d$. Until recently, the bases $\{1 + r_j\}$ were almost exclusively used in the DRM [2, 50]. As we pointed out in [50] $1 + r_j$ are particular cases of *radial basis functions* (RBFs).

$$\varphi_j\left(\mathbf{P}\right) = \varphi_j\left(\left\|\mathbf{P} - \mathbf{P}_j\right\|\right), \quad \varphi : \mathbb{R}^+ \to \mathbb{R}, \quad \varphi(0) \geq 0. \tag{124}$$

Over the past 20 years these functions have been actively investigated in the mathematics and statistics literature for the purpose of

surface fitting [54]. As a result there is now a substantial body of knowledge concerning the theory and application of RBFs for multivariate approximation [54]. One of the consequences of this work is that theory and practice suggest that there are better choices for φ than $\varphi(r) = 1 + r$ [50, 54].

Two of the most popular choices are the *thin plate splines* (TPS) [50]

$$\varphi(r) = r^2 \log r \text{ in } \mathbb{R}^2, \tag{125}$$

$$\varphi(r) = r \text{ in } \mathbb{R}^3, \tag{126}$$

and the multiquadrics (MQs) [11]

$$\varphi(r) = (r^2 + c^2)^{\frac{\beta}{2}}, \quad \beta \text{ an odd integer.} \tag{127}$$

In Eqn. (127) c is an undetermined *shape parameter* [11]. Other choices are higher order splines [54] and Gaussian's [55]. Here we concentrate on TPS and MQs.

In order to satisfy (i)-(iii) one generally needs to modify the representation in Eqn. (117) by the addition of a low order polynomial p_m. Then,

$$\hat{f}(\mathbf{P}) = \sum_{j=1}^{N} a_j \varphi_j(\mathbf{P}) + p_m \tag{128}$$

and

$$u_p(\mathbf{P}) = \sum_{j=1}^{N} a_j \Psi_j(\mathbf{P}) + \chi \tag{129}$$

where $\{\Psi_j\}$ satisfy Eqn. (120) and

$$\mathcal{L}\chi = p_m. \tag{130}$$

For the TPS we add the linear polynomial and

$$p_1 = \begin{cases} ax + by + c, & \text{in } \mathbb{R}^2, \\ ax + by + cz + d, & \text{in } \mathbb{R}^3. \end{cases} \tag{131}$$

For MQs we add $p_0 = a_0$, a constant. Then for TPS interpolation $\{\{a_j\}, a, b, c\}$ and $\{\{a_j\}, a, b, c, d\}$ are obtained from Eqn. (128) with $\mathbf{P} = \mathbf{P}_k, 1 \leq k \leq N$, and the constraints ($\mathbf{P} = (x, y)$)

$$\sum_{j=1}^{N} a_j = \sum_{j=1}^{N} a_j x_j = \sum_{j=1}^{N} a_j y_j = 0 \text{ in } \mathbb{R}^2, \tag{132}$$

and ($\mathbf{P} = (x, y, z)$)

$$\sum_{j=1}^{N} a_j = \sum_{j=1}^{N} a_j x_j = \sum_{j=1}^{N} a_j y_j = \sum_{j=1}^{N} a_j z_j = 0 \text{ in } \mathbb{R}^3. \tag{133}$$

By Duchon's theorem [55, 56], the system Eqn. (128), Eqn. (132) and Eqn. (128), Eqn. (133) have a unique solution if $\{\mathbf{P}_k\}_1^N$ are not colinear in $\mathbb{R}^2$ and $\{\mathbf{P}_k\}_1^N$ are not coplanar in $\mathbb{R}^3$.

Depending on β, one may or may not need the additional p_0 term for MQs. Numerical experimentation suggests that the classical Hardy MQs, $\beta = 1$, have the best approximation properties [57]. In this case we need $p_0 \neq 0$ satisfying [57]

$$\sum_{j=1}^{N} a_j = 0, \tag{134}$$

then Eqn. (128) and Eqn. (134) have a unique solution [55].

One should also note that in order to guarantee the solvability of the collocation equations derived from Eqn. (128) for $1 + r$ in $\mathbb{R}^2$, they should be implemented as [55]

$$\hat{f}(\mathbf{P}) = \sum_{j=1}^{N} a_j r_j + a_0 \tag{135}$$

where $\{a_j\}_1^N$ satisfy Eqn. (134).

At first glance these choices may seem strange since they bear no resemblance to standard bases in $\mathbb{R}$. To remove some of the mystery we observe that TPS are the analogue of one-dimensional cubic splines since they are optimal interpolants in the sense that they minimize the curvature measures

$$\int_{\mathbb{R}^2} \left(\frac{\partial^2 u}{\partial x^2} + 2\frac{\partial^2 u}{\partial x \partial y} + \frac{\partial^2 u}{\partial y^2} \right)^2 dxdy \tag{136}$$

in $\mathbb{R}^2$ or

$$\int_{\mathbb{R}^3} \left(\frac{\partial^2 u}{\partial x^2} + \frac{\partial^2 u}{\partial y^2} + \frac{\partial^2 u}{\partial z^2} + 2\frac{\partial^2 u}{\partial x \partial y} + 2\frac{\partial^2 u}{\partial x \partial z} + 2\frac{\partial^2 u}{\partial y \partial z} \right)^2 dxdydz \tag{137}$$

in $\mathbb{R}^3$.

The MQs were apparently first introduced by Hardy in 1971 [58], but it was not until Franke's paper in 1982 [59] that their remarkable approximation properties came to light. In that paper Franke compared 29 different 2D interpolation methods and based on his criteria the MQs performed the best. In the mathematical and statistical literature TPS and MQs seem to be the most widely used RBFs [54].

Since for $\mathcal{L} = \Delta$, and φ either a TPS or MQ, Ψ can be obtained analytically [2, 11], it is reasonable to choose between them on the basis of their approximation properties. This is a technically difficult problem and until a few years ago not much was known [54]. Here, we quote a number of important results due to Powell [60] and Levesley [61].

Let $\{\mathbf{P}_j\}_1^N$ denote the set of interpolation points and define

$$\delta = \max_{\mathbf{y}\in\mathbb{R}^d} \min_{\mathbf{x}\in\mathbf{X}} \|\mathbf{x}-\mathbf{y}\|, \quad \delta \to 0, N \to \infty. \tag{138}$$

Then it was shown [60] that the TPS interpolant converges uniformly to f in $\mathbb{R}^2$ and if $f \in C^2(D)$ ($\|\cdot\|_\infty = \max_{\mathbf{P}\in D} |f(\mathbf{P})|$)

$$\left\| f - \hat{f} \right\|_\infty \leq c\delta \left|\log \delta\right|, \tag{139}$$

while for $\varphi(r) = r$ [61]

$$\left\| f - \hat{f} \right\|_\infty \leq c\delta^{\frac{1}{2}}. \tag{140}$$

For $f \in C^\infty(D)$ Levesley showed that the MQ interpolant converges *superalgebraically* to f [61]; i.e.,

$$\left\| f - \hat{f} \right\|_\infty \leq c\delta^p, \quad p \geq 1. \tag{141}$$

For certain analytic functions, Madych in [57] showed that the MQ interpolant converges exponentially to f. This latter result has spawned an upsurge of interest in the use of MQ based algorithms for solving PDEs [62-64].

Madych [57] and Beatson and Powell [65] showed under certain conditions on f that the error $\left\| f - \hat{f} \right\|_\infty$ is exponentially decreasing in c, as well as δ, and this property seems to account for much of the efficiency of MQ interpolation. However, this property does not appear to hold for all smooth f's. What has been observed by a number

of researchers is that the error $\left\| f - \hat{f} \right\|_\infty$ seems to decrease initially as c increases and then the error is flat for a range of c and then increases again. Thus there seems to be a range of c where the error is minimized. How to determine the optimal c (c's) numerically is a problem that has been investigated in some detail, but no definitive results seem to be known [11]. In [11], expanding on ideas in [66] we used the statistical technique of *cross-validation* to determine c, but much research needs to be done.

Example 4.1.1 To demonstrate the effectiveness of the MFS-rbf combination for solving Poisson's equation we solve the BVP [11]

$$\Delta u(\mathbf{P}) = 2e^{x-y}, \quad \mathbf{P} = (x, y), \quad \mathbf{P} \in D, \tag{142}$$

$$u(\mathbf{P}) = e^{x-y} + e^x \cos y, \quad \mathbf{P} \in S, \tag{143}$$

where D is the interior of the Oval of Cassini [11]. Its parametric representation is as follows:

$$\begin{cases} x = r(\theta)\cos\theta, \quad y = r(\theta)\sin\theta, \\ r(\theta) = \sqrt{\cos 2\theta + \sqrt{1.1 - \sin^2 2\theta}}, \quad 0 \le \theta \le 2\pi. \end{cases} \tag{144}$$

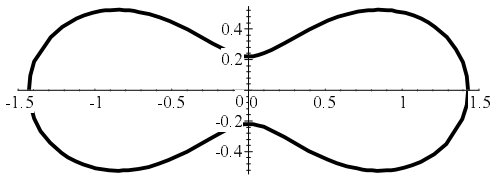

Figure 4. Oval of Cassini.

The solution to Eqn. (142) - Eqn. (143) is given by

$$u(\mathbf{P}) = e^{x-y} + e^x \cos y, \quad \mathbf{P} \in D \cup S. \tag{145}$$

To obtain a particular solution the source term in Eqn. (142) was approximated by MQs using least squares with 33 centers $\{\mathbf{P}_j\}$

and cross-validation was used to determine c [11]. Here, $\{\Psi_j\}$ are computed analytically by [2, 11]

$$\Psi_j = \frac{-c^3}{3}\ln(c\sqrt{r_j^2+c^2}+c^2) + \frac{1}{9}(r_j^2+4c^2\sqrt{r_j^2+c^2}). \qquad (146)$$

For the MFS we use 34 source points

$$\mathbf{Q}_j = (R\cos\theta_j, R\sin\theta_j), \quad \theta_j = \frac{2\pi j}{34}, \quad 1 \le j \le 34, \qquad (147)$$

$R = 12$, and 35 collocation points

$$\mathbf{P}_k = (r(\theta_k)\cos\theta_k, r(\theta_k)\sin\theta_k), \quad \theta_k = \frac{2\pi k}{35}, \quad 1 \le k \le 35. \qquad (148)$$

Using the PRESS statistic we determine that it is reasonable to choose $1 \le c \le 2$ and the solution error appeared to be minimized for $c \simeq 2$.

In Tables 3 - 5 we show results for approximating the source term $2\exp(x-y)$ and the solution u. One easily sees the high accuracy that can be achieved with this method by solving a small number of equations.

Table 3. PRESS statistics.

c	0.8	1.0	2.0	3.0	4.0	5.0
PRESS	2.11	1.34	1.11	2.47	3.63	3.85

Table 4. Absolute error in approximation to $2e^{x-y}$.

x	y	$b(x,y)$	$c=1$	$c=2$	$c=3$	$c=4$	$c=5$
0.0	0.0	2.000	4.44E-4	7.33E-6	2.49E-6	5.02E-6	1.00E-5
0.626	0.0	3.741	1.62E-4	5.29E-6	1.25E-7	1.70E-7	2.11E-5
1.342	0.0	7.653	3.12E-3	2.80E-5	2.71E-5	1.08E-6	3.92E-5
0.174	0.174	2.000	2.16E-4	6.57E-5	3.58E-6	3.78E-6	1.20E-5
0.373	0.373	2.000	2.62E-4	3.67E-5	7.20E-6	1.57E-6	8.49E-6
0.0	0.207	1.626	3.60E-4	8.28E-6	1.87E-6	2.14E-6	6.84E-6
-0.373	0.373	0.949	2.28E-4	1.24E-5	2.88E-6	7.52E-6	5.90E-6
-1.342	0.0	0.523	5.95E-6	1.90E-7	2.18E-6	3.77E-6	7.09E-6

Table 5. Absolute error in approximation to $u(x,y)$.

x	y	$u(x,y)$	$c=1.0$	$c=2.0$	$c=3.0$	$c=4.0$	$c=5.0$
0.0	0.0	2.000	7.86E-7	8.94E-7	5.92E-6	4.48E-5	1.00E-3
0.626	0.0	3.741	5.72E-6	5.25E-8	3.11E-6	2.85E-5	4.48E-2
1.342	0.0	7.653	3.47E-5	2.50E-7	6.23E-6	4.70E-4	7.67E-3
0.174	0.174	2.172	8.82E-6	1.29E-6	5.47E-6	3.59E-5	1.25E-2
0.373	0.373	2.352	1.77E-7	2.13E-6	8.88E-7	8.04E-5	1.55E-2
0.0	0.207	1.792	3.31E-6	3.16E-7	1.66E-6	3.34E-6	2.55E-2
-0.373	0.373	1.116	1.16E-6	4.80E-7	1.60E-6	6.13E-6	7.61E–2
-1.342	0.0	0.523	1.26E-5	2.25E-6	6.29E-5	2.81E-3	7.18E-1

In Example 4.1.3 we will compare these results with TPS and $1+r$ as bases and several other BEMs.

Example 4.1.2 To see that this method extends easily to 3D we consider the problem

$$\Delta u(\mathbf{P}) = 4 - x^2, \quad \mathbf{P} = (x,y,z), \quad \mathbf{P} \in D, \tag{149}$$

$$u(\mathbf{P}) = \frac{-x^4}{12} + y^2 + z^2, \quad \mathbf{P} \in S. \tag{150}$$

where D is the ellipsoid $\left\{(x,y,z) \mid x^2/4 + y^2 + z^2 \leq 1\right\}$ [11]. The exact solution to (149)-(150) is $-x^4/12+y^2+z^2$. A particular solution is obtained by interpolating $4-x^2$ by MQs using 60 basic elements. Again we use the PRESS statistic to determine c. From Table 6 we see that the values $3 \leq c \leq 9$ appear to be acceptable.

Table 6. PRESS statistics.

c	1	3	5	7	9	11	12
PRESS	35.8	0.03	0.15	0.07	0.19	0.8	1.33

As before, $\{\Psi_j\}$ are obtained analytically as [2, 11]

$$\Psi_j(r) = \begin{cases} \dfrac{c^3}{3}, & r = 0, \\ (\dfrac{5c^2}{24} + \dfrac{r_j^2}{12})\sqrt{r_j^2 + c^2} + \dfrac{c^4(\ln(r_j + \sqrt{r_j^2 c^2}) - \ln c)}{8r_j}, & r > 0. \end{cases} \tag{151}$$

For the MFS we use 50 source points uniformly distributed on a sphere of radius 10 and 50 collocation points are uniformly distributed in the polar coordinates (ϕ,θ) on S.

In Table 7 the errors are shown at selected points in D for various values of c. Again we see that errors of $O(10^{-5})$ can be obtained by solving 50 equations. Typical BEMs may require hundreds to thousands of equations to achieve comparable accuracy [2].

Table 7. Absolute error in approximation to $u(x, y, z)$.

x	0.0	1.2	-0.5	-0.7	0.9	0.0	0.4
y	0.0	0.3	0.3	0.5	0.4	-0.5	-0.4
z	0.0	0.1	-0.2	0.2	0.1	0.5	0.21
$u(x, y, z)$	0.00	-0.0728	0.1248	0.2700	0.1153	0.5000	0.2020
$c = 1$	3.6E-4	1.5E-2	2.4E-4	9.9E-3	1.1E-2	4.5E-12	1.6E-3
$c = 3$	1.2E-4	1.4E-3	3.0E-4	5.2E-4	1.1E-3	9.5E-13	4.1E-4
$c = 5$	4.5E-5	9.0E-5	1.4E-4	3.7E-6	2.2E-4	1.1E-12	1.2E-4
$c = 7$	1.7E-5	2.3E-4	7.6E-5	4.6E-6	3.5E-5	7.4E-13	7.6E-5
$c = 9$	9.6E-7	4.0E-4	4.4E-5	1.6E-5	3.2E-5	1.0E-12	7.0E-5
$c = 11$	1.0E-5	5.6E-4	2.5E-5	3.2E-5	7.3E-5	2.3E-12	8.6E-5
$c = 12$	1.6E-5	6.5E-4	1.8E-5	4.3E-5	8.9E-5	4.5E-13	9.8E-5

Example 4.1.3 An interesting extension of the MFS-RBF algorithm for Poisson's equation is its use in approximating solutions to the semilinear equation [12]

$$\Delta u = f(u). \tag{152}$$

Under a variety of conditions on f it can be shown that the Picard iterates $\{u_n\}$ defined by

$$\Delta u_{n+1} = f(u_n), \quad n \geq 0, \tag{153}$$

converge monotonically to u [12]. Since for each n Eqn. (153) is a Poisson equation, we can apply the MFS-RBF algorithm iteratively to solve BVPs for Eqn. (152).

If a fixed number of MFS source points and a fixed number of RBF collocation points are used, the algorithm is relatively inexpensive, since only two LU decompositions are needed to perform the whole process [12].

In [12] Chen used the MFS with TPS to solve blow-up problems for Eqn. (152) with $f(u) = \exp(ku)$. In [67] Chan and Chen extended Chen's algorithm to solve quenching problems for Eqn. (152). (See [67] for a description of the quenching problem.)

Using MQs to find particular solutions, they applied the algorithm to determine the critical major axis a^* of the ellipse

$$\left\{(x,y) \mid \frac{x^2}{a^2} + \frac{y^2}{b^2} \leq 1\right\}$$

with

$$\frac{a}{b} = \frac{1+\exp(-\frac{\pi}{2})}{1-\exp(-\frac{\pi}{2})}$$

for $f(u) = -1/(1-u)$ [67]. Using 16 source points for the MFS and 33 interpolation points for the MQs they found $a^* = 1.471$ (correct to 4 significant figures) in 25 seconds on a GATEWAY 2000 P5-90 personal computer. Previous work by Chan [68] required the use of a parallel supercomputer using traditional integral equation techniques.

4.2 Atkinson's method

To use Atkinson's formula numerically we consider the 2D and 3D cases separately.

In 2D we take $\hat{D}$ to be an ellipse with boundary $B(s) = (a\cos s, b\sin s)$. Making the change of variable

$$\mathbf{Q} = \mathbf{P} + r[B(s) - \mathbf{P}],\ 0 \leq r \leq 1,\ 0 \leq s \leq 2\pi, \tag{154}$$

Eqn. (121) becomes [52]

$$\begin{aligned} \hat{u}(\mathbf{P}) &= \frac{ab}{2\pi}\int_0^{2\pi}\int_0^1 r\ln r K(\mathbf{P};s)\hat{f}(\mathbf{P};r,s)drds \\ &\quad + \frac{ab}{4\pi}\int_0^{2\pi}\int_0^1 rK(\mathbf{P};s)\ln\|B(s)-\mathbf{P}\|^2\,\hat{f}(\mathbf{P};r,s)drds, \\ &= I_1 + I_2, \quad \mathbf{P}\in\overline{D}, \end{aligned} \tag{155}$$

where

$$K(\mathbf{P},s) = 1 - \left[\frac{x}{a}\cos(s) + \frac{y}{b}\sin(s)\right], \quad \mathbf{P} = (x,y), \mathbf{P}\in D, \tag{156}$$

and

$$\hat{f}(\mathbf{P};r,s) \equiv f(\mathbf{P} + r[B(s) - \mathbf{P}]). \tag{157}$$

Because $\mathbf{P} \notin B(s)$, the integrands in I_1 and I_2 are nonsingular, so that standard numerical integration techniques can be used to evaluate them. In [52] Atkinson used product integration rules to do this.

For I_1 Gaussian integration with respect to $-r\ln r$ is used to compute the 'r' integral, while the trapezoidal rule is used to evaluate this 's' integral since the integrand is periodic in s. For I_2 Gaussian integration with respect to 'r' is used to compute the 'r' integral and the trapezoidal rule is used to compute the 's' integral. For smooth integrands $\hat{f}$ the convergence is fast [52].

In $\mathbb{R}^3$, we take $\hat{D}$ to be an ellipsoid with boundary

$$B(\phi,\theta) = (a\cos\phi\sin\theta, b\sin\phi\sin\theta, c\cos\theta), \quad 0 \le \theta \le \pi, \quad 0 \le \phi \le 2\pi \tag{158}$$

where a, b and c are chosen in such a way that $\hat{D} \supset D$. Making the change of variables

$$\mathbf{Q} = \mathbf{P} + r[B(\phi,\theta) - \mathbf{P}], \quad 0 \le r \le 1, \quad 0 \le \theta \le \pi, \quad 0 \le \phi \le 2\pi, \tag{159}$$

in Eqn. (121) it becomes

$$\hat{u}(\mathbf{P}) = -\frac{1}{4\pi}\int_0^{2\pi}\int_0^{\pi}\int_0^{1} rK(\mathbf{P};\phi,\theta)\hat{f}(\mathbf{P};r,\phi,\theta)drd\theta d\phi \tag{160}$$

where

$$\begin{aligned} K(\mathbf{P};\phi,\theta) &= \frac{\sin\theta}{\|B(\phi,\theta)-\mathbf{P}\|}\,(abc - abz\cos\theta \\ &\quad -acy\sin\theta\sin\phi - bcx\sin\theta\cos\phi) \end{aligned} \tag{161}$$

and

$$\hat{f}(\mathbf{P};r,\phi,\theta) = f\left(\mathbf{P} + r[B(\phi,\theta) - \mathbf{P}]\right). \tag{162}$$

In this case, the integrand in Eqn. (160) is nonsingular so that product Gaussian quadrature can be used to approximate Eqn. (160) numerically.

Because Gaussian integration can be costly, particularly if one needs to generate the weights and nodes *on line*, in [69] we used Quasi-Monte Carlo (QMC) integration to evaluate the integrals Eqn. (155) and Eqn. (160). QMC integration is a modification of the classical Monte Carlo approximation I_M of an integral

$$I = \int_{\hat{D}} g(\mathbf{P})dv, \tag{163}$$

by

$$I_M = \frac{V(\hat{D})}{M} \sum_{j=1}^{M} g(\mathbf{P}_j) \tag{164}$$

where $\{\mathbf{P}_j\}_1^M$ are M randomly chosen points in $\hat{D}$ and $V(\hat{D})$ is the area of $\hat{D}$ in $\mathbb{R}^2$ and the volume of $\hat{D}$ in $\mathbb{R}^3$. In QMC integration $\{\mathbf{P}_j\}_1^M$ are quasi-random points as described in [69]. Like Monte Carlo, QMC integration "ignores" singularities in that the convergence rate as $M \to \infty$ is largely independent of the smoothness of g [70], but has a convergence rate $O((\log M)^{d-1}/M), d = 2,3$ [70]. Since the convergence rate is roughly $O(M)$ in $\mathbb{R}^{\,d}, d = 2,3$, we find that choosing $1000 \leq M \leq 3000$ to be adequate for engineering accuracy. Numerical results for Poisson's equation can be found in [69]. In Section 5.1 we will consider the application of this technique to solve inhomogeneous Helmholtz-type equations.

4.3 Some convergence analysis

As indicated in Section 2.4 there has been some convergence analysis of the MFS for Laplace's equations. However, with exception of the partial analysis given in [49, 72] we are unaware of any convergence theorems for Poisson's equation. Here we show how to modify the analysis given in [71] for the traditional DRM to obtain error estimates for the MFS-RBF algorithm based on the estimates Eqn. (39) and Eqn. (110).

To be specific, we consider solving the interior Dirichlet problem

$$\begin{aligned} \triangle u\,(\mathbf{P}) &= f\,(\mathbf{P})\,, \quad \mathbf{P} \in D, & (165)\\ u\,(\mathbf{P}) &= g\,(\mathbf{P})\,, \quad \mathbf{P} \in S, & (166) \end{aligned}$$

in $\mathbb{R}^2$. Let $\hat{u}_p$ be a particular solution to Eqn. (165) obtained by using RBF approximations to f and let $\hat{v}$ be the solution to

$$\begin{aligned} \triangle \hat{v}\,(\mathbf{P}) &= 0, \quad \mathbf{P} \in D, & (167)\\ \hat{v}\,(\mathbf{P}) &= (g - \hat{u}_p)\,(\mathbf{P})\,, \quad \mathbf{P} \in S. & (168) \end{aligned}$$

The BVP in Eqn. (167) - Eqn. (168) is solved by the MFS using $n+1$ sources and the approximation to $\hat{v}$ is denoted by $\hat{v}_n$. Then

$$\hat{w} = \hat{v}_n + \hat{u}_p \tag{169}$$

is the MFS-RBF approximation discussed previously. Defining,

$$\hat{z} = \hat{u}_p + v \tag{170}$$

the error e_n is given by

$$e_n = u - \hat{w} = (u - \hat{z}) + (\hat{z} - \hat{w}). \tag{171}$$

Note as well that $\hat{z}(\mathbf{P}) = 0, \mathbf{P} \in S$. Also, $\hat{z} - \hat{w} = \hat{u}_p + v - \hat{v}_n - \hat{u}_p = \hat{v} - \hat{v}_n$ is the MFS error in approximating $\hat{v}$ by $\hat{v}_n$. This error can be estimated from Eqn. (39) - Eqn. (40). We will return to this matter shortly.

To estimate $u - \hat{z}$ we use a priori estimates for Poisson's equation as in [71]. For this we note that $\Delta(u - \hat{z}) = \Delta u - \Delta \hat{z} = f - \Delta \hat{v} - \Delta \hat{u}_p = f - \hat{f}$, since $\Delta \hat{u}_p = \hat{f}$ by construction of $\hat{u}_p$. Now it is well known that [73],

$$\begin{aligned} \int_D (u - \hat{z})^2 \, dv &\leq c_1 \int_S (u - \hat{z})^2 \, ds + c_2 \int_D \left[\triangle (u - \hat{z})\right]^2 dv \\ &= c_2 \int_D \left(f - \hat{f}\right)^2 dv, \end{aligned} \tag{172}$$

since $u - \hat{z} = 0, \mathbf{P} \in S$.

Now using the L_2 norm, $\|\cdot\|$, on D gives,

$$\|u - \hat{z}\| \leq c \left\| f - \hat{f} \right\| \tag{173}$$

and combining this with Eqn. (171) gives the error bound

$$\|u - \hat{w}\| \leq c \left(\|\hat{v} - \hat{v}_n\| + \left\| f - \hat{f} \right\| \right). \tag{174}$$

To bound $\|\hat{v} - \hat{v}_n\|$ we restrict ourselves to the case where $D = D_r$ is a disc of radius r since we observed in Section 2.4 that the MFS is equivalent to the modified MFS on D_r. Since $\hat{v}$ and $\hat{v}_n$ are harmonic, $\hat{v} - \hat{v}_n$ is harmonic and it follows from the maximum principle that

$$\|\hat{v} - \hat{v}_n\|_{\infty, D_r} \leq \|\hat{v} - \hat{v}_n\|_{\infty, S_r} \tag{175}$$

(S_r is the boundary of D_r). Thus,

$$\|\hat{v} - \hat{v}_n\| = \left[\int_{D_r} (\hat{v} - \hat{v}_n)^2 \, dv \right]^{1/2} \leq \sqrt{\pi} r \, \|\hat{v} - \hat{v}_n\|_{\infty, D_r}. \tag{176}$$

By the Sobolev inequality [27], for $s > 1/2$, $\|\hat{v} - \hat{v}_n\|_{\infty, D_r} \leq c \|\hat{v} - \hat{v}_n\|_s$ where $\|\cdot\|_s$ is the sth Sobolev norm on S_r. From Eqn. (40) we have

$$\|\hat{v} - \hat{v}_n\|_s \leq c\lambda^n \|\hat{v}\|_s , \quad \lambda < 1. \tag{177}$$

For s sufficiently large, $\|\hat{v}\|_s$ can be bounded in terms of the first s derivatives of $\hat{v}$ on S_r. However, $\hat{v} = g - \hat{u}_p$ on S_r so that $\hat{v}^{(k)} = g^{(k)} - \hat{u}_p^{(k)}$ ($u^{(k)}$ is the kth derivative of u). Thus,

$$\|\hat{v}\|_s \leq \|g\|_s + \|\hat{u}_p\|_s \tag{178}$$

so that

$$\|\hat{v} - \hat{v}_n\| \leq c \left[\lambda^n \left(\|g\|_s + \|\hat{u}_p\|_s\right)\right] \tag{179}$$

and

$$\|u - \hat{w}\| \leq c \left(\left\|f - \hat{f}\right\| + \lambda^n \|g\|_s + \lambda^n \|\hat{u}_p\|_s\right) \tag{180}$$

Hence, to obtain convergence rates we need to bound $\|\hat{u}_p\|_s$.

When $\hat{u}_p$ is determined using RBF interpolation one can show that (this is a crude bound)

$$\|\hat{u}_p\|_s \leq c_s N^{3/2} \left\|A^{-1}\right\| \tag{181}$$

where N is the number of basis elements in Eqn. (128), A is the interpolation matrix and $\|\cdot\|$ is spectral norm on matrices. For many rbfs such as TPS and MQs, bounds on $\left\|A^{-1}\right\|$ have been given recently by a number of researchers and a table of known upper bounds is given in [74]. In particular, for MQs we have

$$\left\|A^{-1}\right\| \leq c_{MQ} e^{\mu/\delta}, \mu > 0 \tag{182}$$

where δ is given in Eqn. (138). Hence, for MQ interpolants

$$\|\hat{u}_p\|_s \leq cN^{3/2} e^{\mu/\delta}. \tag{183}$$

Using Eqn. (180) for a given p

$$\|u - \hat{w}\| \leq c \left(\delta^p + \lambda^n \|g\|_s + \lambda^n N^{3/2} e^{\mu/\delta}\right). \tag{184}$$

Suppose δ is chosen so that $\delta = c/N$, then $N^{3/2} e^{\mu/\delta} = N^{3/2} e^{c\mu N} \leq e^{\mu' N}$ for some $\mu' > 0$. For R large enough, $\lambda < e^{-\mu'} < 1$, so that $\lambda^n N^{3/2} e^{\mu/\delta} \leq e^{-n\mu'} e^{N\mu'} \leq e^{-(N-n)\mu'} = \left(e^{-\mu'}\right)^{(n-N)}$. Choosing

$n = \beta N$, $\beta > 1$, the last term in Eqn. (184) is bounded by $(\lambda')^N$, $0 \leq \lambda' < 1$. Hence, as $N \to \infty$, the convergence of the MFS-MQ is superalgebraic. For other RBFs, such as TPS, the error will be dominated by the approximation error $\left\| f - \hat{f} \right\|$ so that convergence is expected to be slower than for MQs.

Example 4.3.1 To see the effect of using different RBFs to approximate f and to compare the MFS to several standard BEMs we solve Eqn. (142) - Eqn. (143) using three RBFs - $1 + r$, TPS and MQs and three different solution methods for the homogeneous problem - MFS, a standard BEM with quadratic elements [1] and an adaptive spectrally convergent Nyström method developed by Jeon and Atkinson [75] using the trapezoidal rule to discretize the double layer integral equation for Eqn. (142) - Eqn. (143).

In Fig. 5 we show graphs of the absolute values of the errors $|u - u_n|$ on the x axis. This shows the results of solving Eqn. (142) - Eqn. (143) by a quadratic BEM using 32 elements with the source term approximated by RBF interpolation using 60 quasi-random points. We choose the shape parameter c of the MQ to be 0.1. One can see from these graphs that, as expected, there is little difference among the errors of $1+r$, TPS and MQs, although TPS and MQs are somewhat more accurate than $1 + r$. This situation is characteristic of engineering studies and our results seem to be consistent with those of [76, 77].

In Figs. 6 and 7 we show the results of solving Eqn. (142) - Eqn. (143) using Jeon and Atkinson's adaptive program. Here we requested an error of 10^{-5} and again the RBFs were interpolated using 60 quasi-random points. The shape parameter of the MQ is chosen to be 0.7. Here as expected from our previous discussion, $1+r$ and TPS perform in a similar fashion but MQs behave substantially better - reflecting the spectral convergence of both Atkinson's algorithm and MQ interpolation.

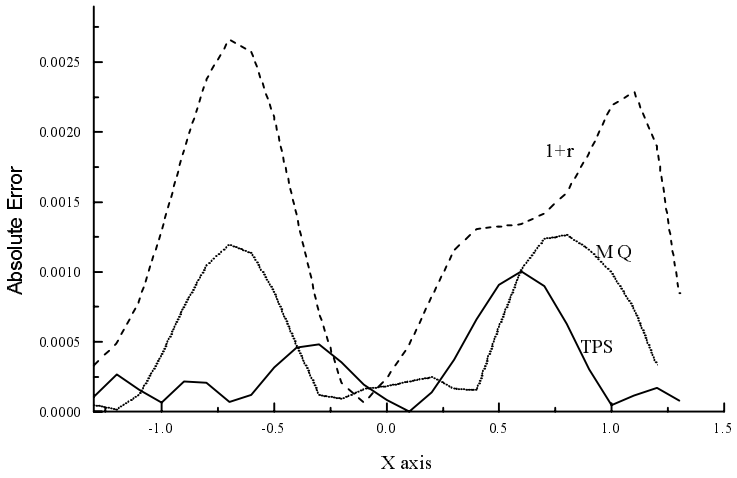

Figure 5. Absolute errors along x-axis using quadratic BEM.

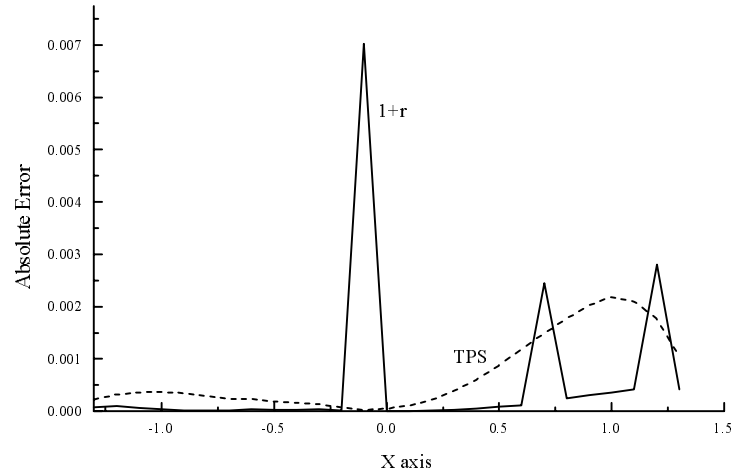

Figure 6. Absolute errors along x-axis using BIE.

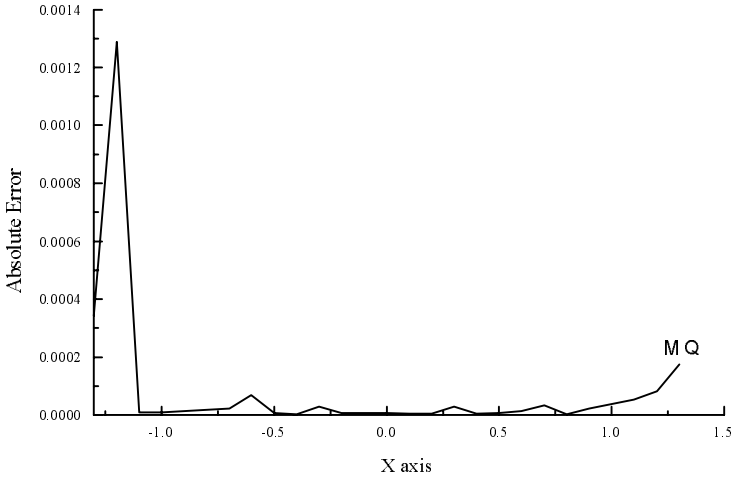

Figure 7. Absolute errors along x-axis using BIE.

The results of solving Eqn. (142) - Eqn. (143) by the MFS are shown in Figs. 9 and 10. Here we used 34 source points uniformly distributed around a circle of radius 10. As shown in Fig. 8, we choose 35 uniformly distributed (in terms of angle) collocation points on the physical boundary. The shape parameter c of the MQ is chosen to be 2.5. Again MQs performed substantially better than both TPS and $1 + r$, although, as expected, TPS outperforms $1 + r$. As discussed previously, this again reflects the spectral convergence of the MFS-MQ combination.

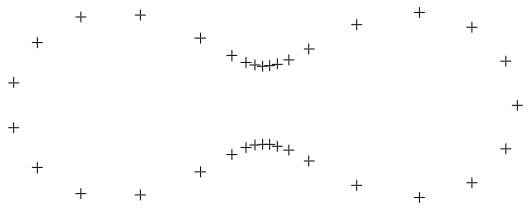

Figure 8. 35 collocation points on the physical boundary.

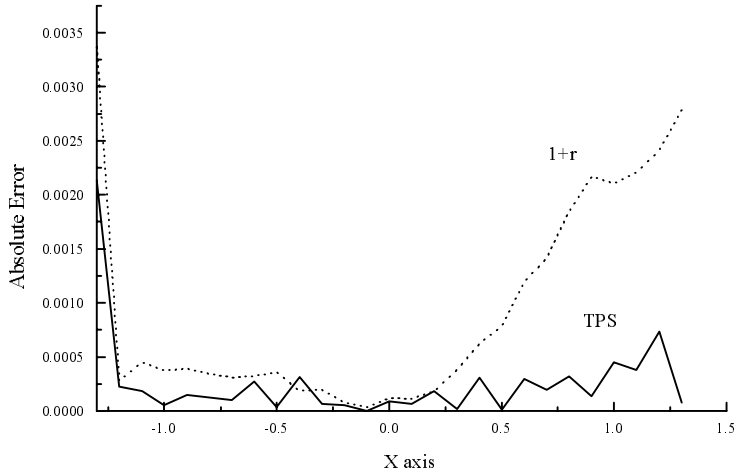

Figure 9. Absolute errors along x-axis using MFS.

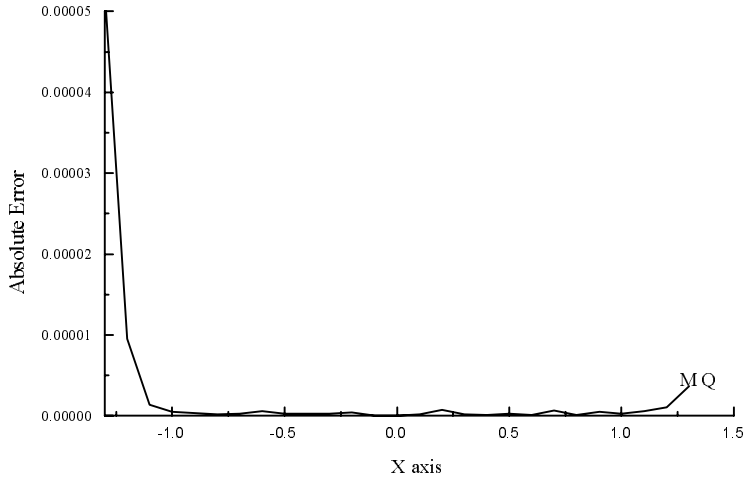

Figure 10. Absolute errors along x-axis using MFS-MQ.

5 The MFS for the diffusion equation

Encouraged by the success of the MFS for solving elliptic problems we have been motivated to extend the method to solve time-dependent diffusion problems. This is an area that appears to have been largely neglected in the MFS literature and we are aware of only two published numerical studies of this problem. In [78] DeMey consid-

ered solving the one-dimensional heat equation using time-dependent sources and this approach was generalized to 2D problems by Walker in [79].

Since using time-dependent sources can be quite cumbersome [78-79], we have begun to examine the use of the Laplace transform (LT) [2] to remove the time-dependence. This converts the BVP to an equivalent elliptic problem which can be solved by the MFS as before. The time-dependence is then restored by numerical inversion of the transform. Although this was one of the first approaches taken in the BEM literature to solve the diffusion equation [80, 81], its accuracy was hampered by poor inversion techniques [81]. As LT inversion is an ill-posed problem, small truncation errors can be greatly magnified in the inversion process leading to poor numerical results. However, in recent years this method has been re-examined using a more sophisticated inversion algorithm due to Stehfest [81] and the results have been encouraging. This interest seems to have been rekindled by the paper of Moridis and Reddell [82] and has been further developed by Zhu *et al* [24], Satravaha [83] and Zu and Satravaha [84]. The results in [24, 82-83] suggested to us that coupling the MFS with the LT could provide an efficient algorithm.

Letting D be as in Section 2 we consider the initial-BVP:

$$\frac{1}{k}\frac{\partial u(\mathbf{P},t)}{\partial t} = \Delta u(\mathbf{P},t), \quad \mathbf{P} \in D, \quad t > 0, \tag{185}$$

with boundary conditions

$$u(\mathbf{P},t) = g_1(\mathbf{P},t), \quad \mathbf{P} \in S_1, \quad t > 0, \tag{186}$$

$$\frac{\partial u(\mathbf{P},t)}{\partial n_{\mathbf{P}}} = g_2(\mathbf{P},t), \quad \mathbf{P} \in S_2, \quad t > 0, \tag{187}$$

$S_1 \cap S_2 = \emptyset, S_1 \cup S_2 = S$, and initial condition

$$u(\mathbf{P},0) = u_0(\mathbf{P}), \quad \mathbf{P} \in D \cup S. \tag{188}$$

The diffusion coefficient k is constant and u_0, g_1 and g_2 are given functions.

To solve Eqn. (185) - Eqn. (188) numerically, we use the Laplace transform

$$\mathbf{L}\left[u(\mathbf{P},t)\right] \equiv U(\mathbf{P};s) = \int_0^\infty u(\mathbf{P},t)e^{-st}dt \tag{189}$$

for $s \in \mathbb{R}, s > M$, to remove the time-dependence in Eqn. (185) - Eqn. (187). Applying $\mathbf{L}$ to both sides of Eqn. (185) using

$$\mathbf{L}\left[\frac{\partial u(\mathbf{P},t)}{\partial t}\right] = sU(\mathbf{P};s) - u_0(\mathbf{P}) \tag{190}$$

gives U as to solution to the transformed problem

$$\begin{aligned}
\left(\Delta - \frac{s}{k}\right) U(\mathbf{P};s) &= -\frac{u_0(\mathbf{P})}{k}, \quad \mathbf{P} \in D, && (191)\\
U(\mathbf{P};s) &= G_1(\mathbf{P};s), \quad \mathbf{P} \in S_1, && (192)\\
\frac{\partial U(\mathbf{P};s)}{\partial n_{\mathbf{P}}} &= G_2(\mathbf{P};s), \quad \mathbf{P} \in S_2, && (193)
\end{aligned}$$

where

$$G_i(\mathbf{P};s) = \mathbf{L}\left(g_i\right), \quad i = 1,2. \tag{194}$$

Now for each $s > M$ Eqn. (191) - Eqn. (193) is a BVP for the modified Helmholtz operator $\Delta - \lambda^2, \lambda = \sqrt{s/k}$ and for each λ Eqn. (191) - Eqn. (193) can be solved using the BEM [24]. In [16] we introduced the MFS to obtain U. Having done this, in principle, one can obtain $u(\mathbf{P},t)$ by

$$u(\mathbf{P},t) = \mathbf{L}^{-1}(U) \tag{195}$$

where $\mathbf{L}^{-1}$ is the inverse LT. Practically, we will only be able to obtain $U(\mathbf{P};s)$ for a finite number of values $\{s_i\}$ and then some numerical technique has to be employed to approximate $\mathbf{L}^{-1}(U)$. We return to this in Section 5.2. For now we concentrate on solving Eqn. (191) - Eqn. (193).

Let U_p be a particular solution to $\left(\Delta - \lambda^2\right) u = -u_0/k \equiv f$, then $V = U - U_p$ satisfies

$$\begin{aligned}
\left(\Delta - \lambda^2\right) V(\mathbf{P};s) &= 0, \quad \mathbf{P} \in D, && (196)\\
V(\mathbf{P};s) &= G_1(\mathbf{P};s) - U_p(\mathbf{P}), \quad \mathbf{P} \in S_1, && (197)\\
\frac{\partial V(\mathbf{P};s)}{\partial n_{\mathbf{P}}} &= G_2(\mathbf{P};s) - \frac{\partial U_p(\mathbf{P})}{\partial n_{\mathbf{P}}}, \quad \mathbf{P} \in S_2, && (198)
\end{aligned}$$

Let

$$G(\mathbf{P},\mathbf{Q};\lambda) = \begin{cases} \dfrac{-1}{2\pi} K_0\left(\lambda r\right), & (\mathbf{P},\mathbf{Q}) \in \mathbb{R}^2, \\ \dfrac{-1}{4\pi r} \exp\left(-\lambda r\right), & (\mathbf{P},\mathbf{Q}) \in \mathbb{R}^3, \end{cases} \tag{199}$$

$r = \|\mathbf{P} - \mathbf{Q}\|$, be the fundamental solution of $\Delta - \lambda^2$ in $\mathbb{R}^d, d = 2, 3$ (K_0 is the Bessel function of the second kind and order zero). Then, in analogy to the Helmholtz equation, we consider approximations V_n of V of the form

$$V_n = \sum_{j=1}^{n} a_j G(\mathbf{P}, \mathbf{Q}_j) \tag{200}$$

where $\{\mathbf{Q}_j\}_1^n$ are n source points on a surface $\hat{S}$ in the exterior of D. As before, $\{a_j\}_1^n$ can be determined either by collocation or least squares. We consider only collocation in the remainder of this section. Having done this, we define

$$\mathcal{U}_n = V_n + U_p \tag{201}$$

as an approximation to U. As for Poisson's equation, we need to determine U_p or an approximation to it.

Based on our work for Poisson's equation, it is reasonable to use a method based on a approximating f by RBFs. However, it appears difficult to analytically solve the equations

$$\left(\Delta - \lambda^2\right) \Psi_j = \varphi_j \tag{202}$$

for important cases of φ. Zhu [85] considered this problem for $\varphi(r) = r^m, m \geq 0$, in $\mathbb{R}^2$. Using properties of the Bessel functions he was able to obtain recursion relations in m for the Ψ's, but no explicit formulas were given. For MQs we have been unable to obtain analytic formulas as well, although it is possible to find integral formulas using the variation of parameters formula for ODEs [2]. As a consequence, in [16] we adopted an approach using Atkinson's formula, but this can still be quite time consuming. In [86] Chen and Rashed obtained analytic particular solutions when φ_j in Eqn. (202) was a thin plate spline. The derivation in [86] was heuristic and a systematic derivation was given in [26]. The procedure given in [26] enables one to compute particular solutions for higher order splines as well. We will discuss this in Section 5.3. For now, we consider the use of Atkinson's formula.

5.1 Atkinson's formula

As we noted in Section 4, a particular solution U_p of $(\Delta - \lambda^2)U = f$ is given by

$$U_p(\mathbf{P};\lambda) = \int_{\hat{D}} G(\mathbf{P},\mathbf{Q};\lambda) f(\mathbf{Q}) dv, \quad \mathbf{P} \in D \cup S. \tag{203}$$

Using the change of variables given in Section 4.2, the formula for U_p Eqn. (203) can be converted to integrals which can be evaluated as proposed there. In $\mathbb{R}^3$ the transformed integrand is nonsingular. In $\mathbb{R}^2$, since

$$K_0(\lambda r) = -\log \|\mathbf{P} - \mathbf{Q}\| + k_0(r) \tag{204}$$

where k_0 is analytic [87],

$$\begin{aligned} \int_{\hat{D}} G(\mathbf{P},\mathbf{Q};s) f(\mathbf{Q}) dv &= \frac{-1}{2\pi} \left[\int_{\hat{D}} \log \|\mathbf{P} - \mathbf{Q}\| f(\mathbf{Q}) dv \right. \\ &\quad \left. + \int_{\hat{D}} k_0 (\|\mathbf{P} - \mathbf{Q}\|) f(\mathbf{Q}) dv \right]. \end{aligned} \tag{205}$$

The first integral in Eqn. (205) is the same as in Eqn. (155) and can be approximated by Atkinson's method. The second integral is regular and can be evaluated by a product Gauss-trapezoidal rule. However, to simplify programming we used the QMC method as discussed in Section 4.2. In future work we expect to compare this method with the use of Gaussian product rules and approximation of f by splines. (However, see Example 5.3.1.3.)

If $\hat{U}_p$ denotes the particular solution given by approximating Eqn. (203) by QMC integration, then

$$\hat{W} = \hat{V}_n + \hat{U}_p \tag{206}$$

where $\hat{V}_n$ is the MFS approximation to V with U_p in Eqn. (197) - Eqn. (198) replaced by $\hat{U}_p$. We refer to this technique as the *Las Vegas Method* [16].

5.2 The inverse Laplace transform

To evaluate $\mathbf{L}^{-1}(\hat{W})$, $\hat{W}$ is computed at a finite number of points

$$s\nu = \frac{\ln 2}{t}\nu, \quad \nu = 1, 2, \cdots, n_s, \tag{207}$$

where 't' is the time at which the solution to Eqn. (185) - Eqn. (188) is desired. Following recent work by Zhu *et al* [83, 84] we used Stehfest's method to approximate $\mathbf{L}^{-1}(\hat{W})$. This is given by [81] ($\widehat{u}(\mathbf{P},t)$ is the approximation to $u(\mathbf{P},t)$)

$$\widehat{u}(\mathbf{P},t) = \frac{\ln 2}{t}\sum_{\nu=1}^{n_s} W\nu\widehat{W}(\mathbf{P};s\nu) \tag{208}$$

where

$$W\nu = (-1)^{\frac{n_s}{2}+\nu}\sum_{k=\frac{1}{2}(\nu+1)}^{\min\{\nu,\frac{n_s}{2}\}} \frac{k^{\frac{n_s}{2}}(2k)!}{(\frac{n}{2}-k)!k!(k-1)!(\nu-k)!(2k-\nu)!}. \tag{209}$$

The accuracy of Eqn. (208) - Eqn. (209) depends on the correct choice of n_s. As n_s increases, the accuracy improves and then round-off error becomes a factor and eventually the accuracy declines [81]. This is a manifestation of the ill-posedness of LT inversion. As we shall see, the optimal value of n_s has a significant effect on our proposed method. In [81] Stehfest tested Eqn. (208) - Eqn. (209) on 50 functions with known inverse transforms and concluded that the optimal value of n_s is 10 for single precision variables and $n_s = 18$ for double precision variables. In previous work using traditional BEMs, Moridis and Reddell [82] and Zhu *et al* [24, 83-84] found no significant differences in their results for $6 \leq n_s \leq 10$.

5.2.1 Numerical examples

To test our method we solved problems discussed in [24] and [82]. Computations were performed on the same PC as Section 4.1. We use Microsoft IMSL Mathematical and Statistical Libraries (FORTRAN Subroutines Version 2.0) to evaluate $K_{\mathbf{0}}$.

Example 5.2.1.1 We consider the flow of heat in the square $[-0.2, 0.2]$ $\times$ $[-0.2, 0.2]$ (units are in meters) with $u_{\mathbf{0}} = 1$ and Dirichlet boundary

conditions $u(\mathbf{P},t) = 0, \mathbf{P} \in S$. The analytic solution of this problem is [88]

$$u(\mathbf{P},t) = \frac{16}{\pi^2} \sum_{n=0}^{\infty} \sum_{m=0}^{\infty} L_{n,m} \cos \frac{(2n+1)\pi x}{2a} \cos \frac{(2m+1)\pi y}{2a} \exp(-D_{n,m} t) \tag{210}$$

where $a = 0.2$,

$$L_{n,m} = \frac{(-1)^{n+m}}{(2n+1)(2m+1)} \text{ and } D_{n,m} = \frac{k\pi^2}{4} \left[\frac{(2n+1)^2}{a^2} + \frac{(2m+1)^2}{a^2} \right]. \tag{211}$$

Here k is the thermal diffusivity of the substance.

In order to compare our result with those in [24, 82], we chose the same thermal diffusivity $k = 5.8 \times 10^{-7}$ and observation time $t = 9000$ seconds. The temperature distribution was calculated along the x axis at $y = 0.025$. For the MFS we chose 16 equally spaced collocation points (see Fig. 11) on the boundary and the same number of source points equally spaced on a circle of radius $r = 3.0$ with center $(0, 0)$. The particular solution Eqn. (203) was evaluated using QMC integration with 1000 quasi-random nodes.

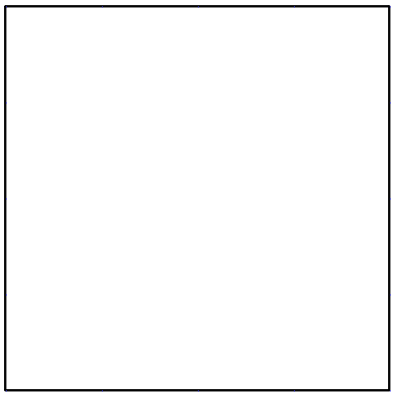

Figure 11. Collocation points on the boundary for the MFS.

As shown in Fig. 12, for the Las Vegas method the errors between the analytical and numerical solutions are virtually unnoticeable for

the case $n_s \geq 8$ with maximum errors of $O(10^{-4})$ for $n \geq 10$. In contrast to the behavior reported in [24, 82], the accuracy of the Las Vegas method increased substantially as n_s increased from 6 to 10. The maximum error of the Las Vegas method was 1.8×10^{-4} for $n_s \geq 12$.

To see the effect of numerical integration, we observe that since $u_0 = 1$ is harmonic, the solution can be calculated without numerical integration. In fact, if $z = u - u_0$, then $z_t = u_t = \Delta u = \Delta(z + u_0) = \Delta z + \Delta u_0 = \Delta z$. Thus z satisfies the homogeneous diffusion equation with zero initial condition which can be solved as before.

The results for various n_s of doing this are shown in Figs. 12-13. As one can see, there is little difference in the accuracy of the two methods.

For curiosity, we compared the Las Vegas method with the classical Monte Carlo method with 1000 randomly chosen nodes. The results are shown in Fig. 14. The effect of using QMC integration rather than MC integration is substantial, which is consistent with the $O(M^{-1} \log M)$ error of QMC integration and the $O(M^{-1/2})$ error of MC integration.

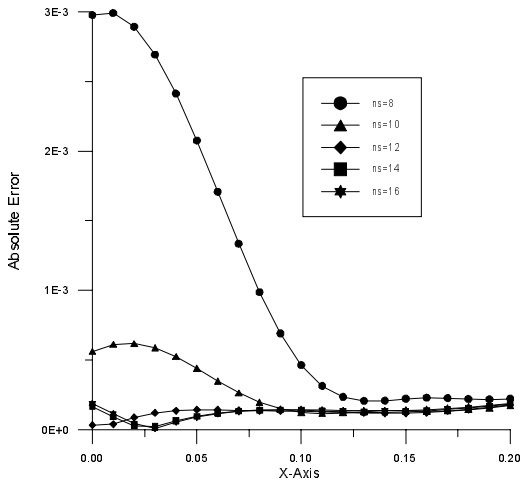

Figure 12. MFS error with numerical integration.

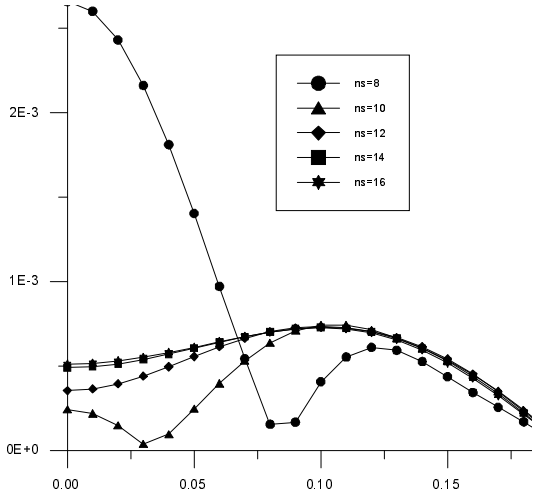

Figure 13. MFS error without numerical integration.

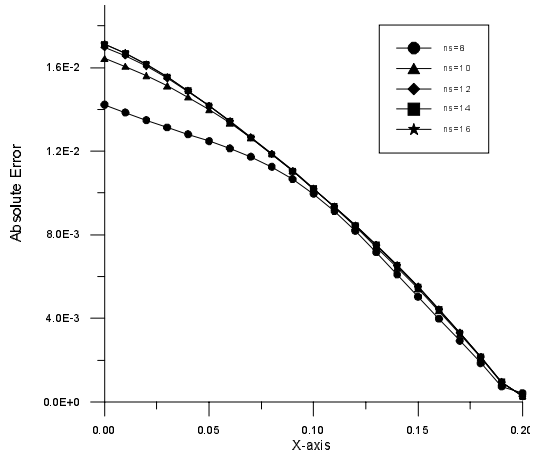

Figure 14. MFS error with Monte Carlo integration.

Example 5.2.1.2. To see that the Las Vegas method can be applied in 3D we considered a generalization of the problem in Example 5.1 [16]. Here we take D to be a cube of side 0.2 (meters) $u_{\mathbf{0}} = 1$ and zero Dirichlet boundary conditions. The analytic solution is [88] ($\mathbf{P} = (x, y, z)$)

$$u(\mathbf{P}, t) = \frac{64}{\pi^3} \sum_{n=0}^{\infty} \sum_{m=0}^{\infty} \sum_{\ell=0}^{\infty} \frac{(-1)^{n+m+\ell}}{(2n+1)(2m+1)(2\ell+1)} \exp(-D_{n,m,\ell} t) \times \cos \frac{(2n+1)\pi x}{2a} \cos \frac{(2m+1)\pi y}{2b} \cos \frac{(2\ell+1)\pi z}{2c}$$

where $a = b = c = 0.2$ and

$$D_{n,m} = \frac{k\pi^2}{4}\left[\frac{(2n+1)^2}{a^2} + \frac{(2m+1)^2}{b^2} + \frac{(2\ell+1)^2}{c^2}\right].$$

The thermal diffusivity k and observation time t are the same as in Example 5.1. The temperature distribution was calculated along the x axis at $y = 0.025$ and $z = 0.08$.

For the MFS we chose 62 collocation points distributed on each side of the cube as shown in Fig. 15 and the same number of source points distributed in the same fashion on the surface of a cube of side three. To evaluate the particular solution we used QMC integration with 2000 points. Results of this calculation as a function of n_s are shown in Fig. 16. In Fig. 17 we show the result of subtracting off $u_0 = 1$.

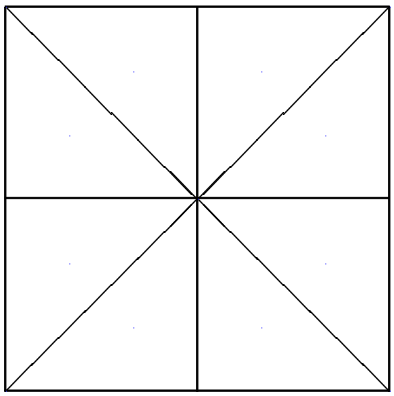

Figure 15. Collocation points on each surface of the cube.

A curious effect of the Las Vegas method is that solving the 3D problem is generally more efficient than solving the 2D one. In Table 8 we show CPU times (in seconds), using a 486 PC, needed to calculate the solution at an interior point for various values of n_s. The reason for this is traceable to the fact that the 2D fundamental solution is a Bessel function, which is a substantially more expensive to evaluate than the exponential in 3D.

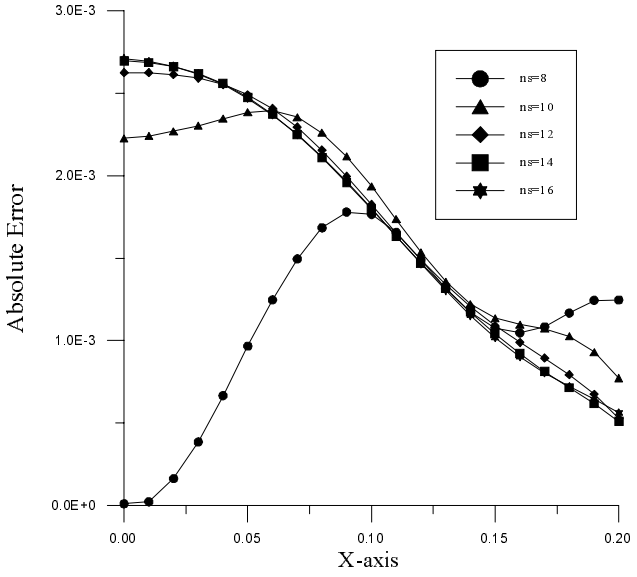

Figure 16. MFS error with numerical integration.

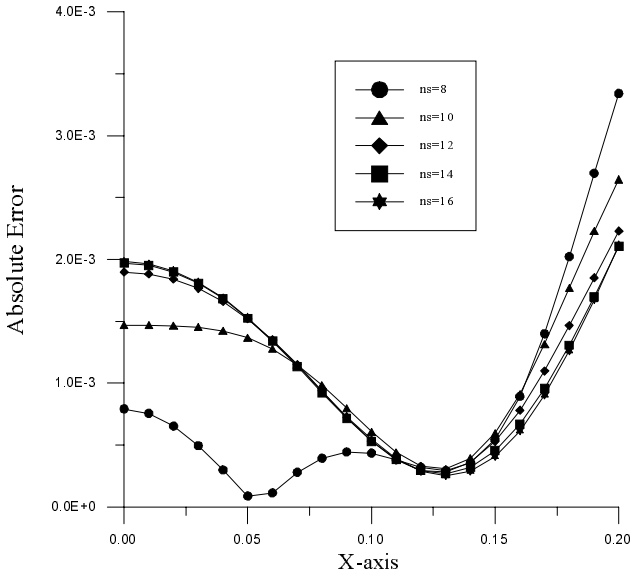

Figure 17. MFS error without numerical integration.

Table 8. Comparison of CPU times for Examples 5.1 and 5.2.

n_s	CPU (seconds)	
	2D	3D
8	29.11	13.07
10	36.03	16.37
12	43.06	19.60
14	49.93	22.85
16	56.85	26.09

5.3 Particular solutions using TPS

In general, we expect the RBF approach to finding particular solutions to be more efficient than Atkinson's formula. However, as we have already pointed out, this approach appears to be difficult, since solving Eqn. (202) analytically is apparently not possible for many important RBFs. However, if φ is a TPS, then Eqn. (202) can be solved by a generalization of the well-known annihilator method used for ODEs [89]. This follows because $\Delta^2\varphi = 0, \mathbf{P} \neq \mathbf{0}$, if φ is a TPS [55]. For clarity, we consider the 2D and 3D cases separately.

In 2D, $\varphi(r) = r^2 \log r$ so that Ψ is obtained by solving

$$(\Delta - \lambda^2)\Psi = r^2 \log r. \tag{212}$$

Applying Δ^2 to both sides of Eqn. (212) using $\Delta^2 \left(r^2 \log r\right) = 0, r > 0$, gives

$$\Delta^2(\Delta - \lambda^2)\Psi = 0. \tag{213}$$

Since $r^2 \log r$ is radial, we look for radial solutions of Eqn. (213). Letting

$$\Delta_r = \frac{1}{r}\frac{d}{dr}(r\frac{d}{dr}) = \frac{d^2}{dr^2} + \frac{1}{r}\frac{d}{dr} \tag{214}$$

be the radial part of the Laplacian, radial solutions $\Psi(r)$ of Eqn. (214) satisfy

$$\Delta_r^2(\Delta_r - \lambda^2)\Psi = 0. \tag{215}$$

Using the fact that Δ_r^2 and $\Delta_r - \lambda^2$ commute, we can write [26]

$$\Psi = v + w \tag{216}$$

where

$$(\Delta_r - \lambda^2)w = 0 \tag{217}$$

and

$$\Delta_r^2 v = 0. \tag{218}$$

As is well known, Eqn. (217) is a Bessel equation whose general solution is [89]

$$w = AI_0(\lambda r) + BK_0(\lambda r) \tag{219}$$

where I_0 is a Bessel function of the first kind and order zero and K_0 is as before.

By straightforward algebra we find that Eqn. (218) is equivalent to the *Euler equation*

$$r^4 \frac{d^4 v}{dr^4} + 2r^3 \frac{d^3 v}{dr^3} - r^2 \frac{d^2 v}{dr^2} + r \frac{dv}{dr} = 0, \tag{220}$$

whose characteristic polynomial is $p^2(p-2)^2$ [89]. Thus it follows that [89]

$$v = a + b \log r + cr^2 + dr^2 \log r. \tag{221}$$

Hence,

$$\Psi = AI_0(\lambda r) + BK_0(\lambda r) + a + b \log r + cr^2 + dr^2 \log r. \tag{222}$$

To determine the constants in Eqn. (222) we make use of the fact that $\left(\Delta_r - \lambda^2\right) \Psi = r^2 \log r$ to guarantee that Ψ is a particular solution. Using

$$\left(\Delta_r - \lambda^2\right) I_0 = \left(\Delta_r - \lambda^2\right) K_0 = 0,$$

some tedious algebra then gives [26]

$$a = \frac{-4}{\lambda^2}, \quad b = \frac{-4}{\lambda^4}, \quad c = 0, \quad d = \frac{-1}{\lambda^2}. \tag{223}$$

Thus,

$$\Psi = AI_0(\lambda r) + BK_0(\lambda r) - \frac{4}{\lambda^2} - \frac{4 \log r}{\lambda^4} - \frac{r^2 \log r}{\lambda^2} \tag{224}$$

is a particular solution. Usually we want particular solutions which are continuous at $r = 0$ and this can be done by choosing B to cancel the '$\log r$' term in K_0. Using $K_0(\lambda r) \to -\gamma - \log(\lambda r/2), r \to 0$, ($\gamma \simeq 0.5772156649015328$ is Euler's constant [87]) gives $B = -4/\lambda^4$.

Now, except for I_0, Eqn. (224) agrees with Eqn. (15) in [86]. However, since particular solutions are not unique we choose $A = 0$ for simplicity. Hence,

$$\Psi = \begin{cases} -\frac{4}{\lambda^2} - \frac{4\log r}{\lambda^4} - \frac{r^2\log r}{\lambda^2} - \frac{4K_0(\lambda r)}{\lambda^4}, & r \neq 0, \\ -\frac{4}{\lambda^2} - \frac{4\gamma}{\lambda^4} + \frac{4}{\lambda^4}\log\left(\frac{\lambda}{2}\right) & r = 0. \end{cases} \tag{225}$$

As noted in Section 4.1 we also need to solve $\left(\Delta - \lambda^2\right)\chi = ax + by + c$ to obtain particular solutions for the linear term in Eqn. (128). This can be done by undetermined coefficients [2] giving

$$\chi = -\frac{1}{\lambda^2}(ax + by + c). \tag{226}$$

In $\mathbb{R}^3$, $\varphi(r) = r$ and again $\Delta^2\varphi = 0, r > 0$. Using this, radial particular solutions for $\left(\Delta - \lambda^2\right)\Psi = r$ can be obtained by solving

$$\Delta_r^2\left(\Delta_r - \lambda^2\right)\Psi = 0 \tag{227}$$

where

$$\Delta_r = \frac{1}{r^2}\frac{d}{dr}\left(r^2\frac{d}{dr}\right) = \left(\frac{d^2}{dr^2} + \frac{2}{r}\frac{d}{dr}\right). \tag{228}$$

As before,

$$\Psi = v + w \tag{229}$$

where

$$\left(\Delta_r - \lambda^2\right)w = 0 \tag{230}$$

and

$$\Delta_r^2 v = 0. \tag{231}$$

To solve Eqn. (231), let $w = z/r$, then z satisfies

$$\frac{d^2z}{dr^2} - \lambda^2 z = 0, \tag{232}$$

so that

$$w = \frac{Ae^{-\lambda r}}{r} + \frac{Be^{\lambda r}}{r}. \tag{233}$$

To solve Eqn. (231), we note that it is equivalent to the Euler equation

$$r^4\frac{d^4v}{dr^4}+4r^3\frac{d^3v}{dr^3}=0 \tag{234}$$

whose characteristic polynomial is $(p+1)p(p-1)(p-2)$. Hence,

$$v=a+br+\frac{c}{r}+dr^2, \tag{235}$$

so that

$$\Psi=\frac{Ae^{-\lambda r}}{r}+\frac{Be^{\lambda r}}{r}+a+br+\frac{c}{r}+dr^2. \tag{236}$$

Using $\left(\Delta-\lambda^2\right)\Psi=r$ and some algebra gives

$$a=d=0,\quad b=\frac{-1}{\lambda^2},\quad c=\frac{-2}{\lambda^4}. \tag{237}$$

For continuous particular solutions we choose $A=2/\lambda^4, B=0$ giving

$$\Psi=\begin{cases}-\dfrac{r}{\lambda^2}-\dfrac{2}{\lambda^4 r}+\dfrac{2e^{-\lambda r}}{\lambda^4 r}, & r>0,\\ \dfrac{-2}{\lambda^3}, & r=0,\end{cases} \tag{238}$$

This agrees with Eqn. (28) in [86].

As for the 2D case χ in Eqn. (129) it can be determined by solving $\left(\Delta-\lambda^2\right)\chi=ax+by+c+d$ giving

$$\chi=-\frac{1}{\lambda^2}\left(ax+by+cz+d\right). \tag{239}$$

One can now use these expressions to obtain approximate particular solutions for $\left(\Delta-\lambda^2\right)u=f$ when f is approximated by TPS.

Last, we note that this procedure can be extended to find particular solutions when φ is a higher order spline; i.e.,

$$\varphi_m(r)=r^{2m-2}\log r,\quad m\geq 2 \text{ in } \mathbb{R}^2, \tag{240}$$

and

$$\varphi_m(r)=r^{2m-3},\quad m\geq 2 \text{ in } \mathbb{R}^3. \tag{241}$$

Since $\Delta^m\varphi_m=0$, the annihilator method can be used again, but a symbolic program is probably necessary to do the algebra.

5.3.1 Numerical examples

Example 5.3.1.1 To test the TPS algorithm for solving the modified Helmholtz equation we solved the boundary value problem

$$\Delta u - ku = 4 - k(x^2 + y^2), \quad (x, y) \in D, \tag{242}$$

$$u = x^2 + y^2, \quad (x, y) \in S, \tag{243}$$

where $k > 0, D$ is the unit square and S its boundary. The exact solution is $u = x^2 + y^2$.

To interpolate $4 - k(x^2 + y^2)$, we chose 36 and 49 uniformly distributed grid points in $D \cup S$. For the MFS we chose 16 evenly spaced collocation points on S and the same number of source points on a circle with center $(0.5, 0.5)$ and radius 10. Relative errors observed along $y = 0.5$ for various values of k are shown in Fig. 18.

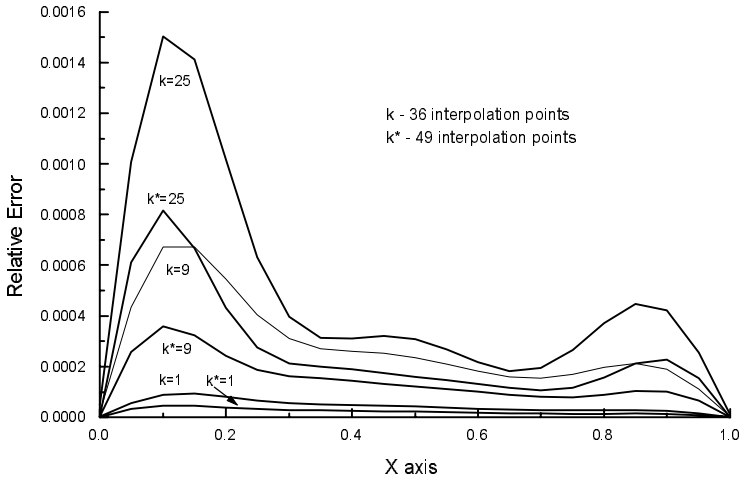

Figure 18. Relative errors for various k and interpolation points.

To demonstrate the efficiency of our version of LTDRM, we used the same problems in Examples 5.2.1.1 and 5.2.2.2 and compared our results with the Las Vegas method and the LTDRM in [24] and the LTBEM in [82].

Example 5.3.1.2 The description of this example is exactly the same as in Example 5.1. For purposes of comparison, we choose the same collocation points and source points as in Example 5.2.1.1.

To find a particular solution, we need to interpolate the forcing term of Eqn. (191) by TPS. Notice that in this case the forcing term becomes extremely simple, a constant. It is well known that a constant function can be exactly approximated by TPS. In this case no interior points are required for the purpose of reconstructing the forcing term. Hence, we choose the same 16 collocation points which are used in the MFS as interpolation points (see Fig. 11).

In Fig. 19 we denote $ns = n_s$ and $\bullet$ stands for the absolute error of the LTDRM and solid lines the absolute error of LTMFS for various n_s. As shown in Fig. 19, both the absolute error of the LTDRM and LTMFS are bounded by 7×10^{-4} for $n_s \geq 10$. With increasing n_s the absolute error becomes stable. The accuracy of our proposed method is similar to the Las Vegas method in Example 5.2.1.1 and far superior to the LTDRM in [24] and the LTBEM in [82].

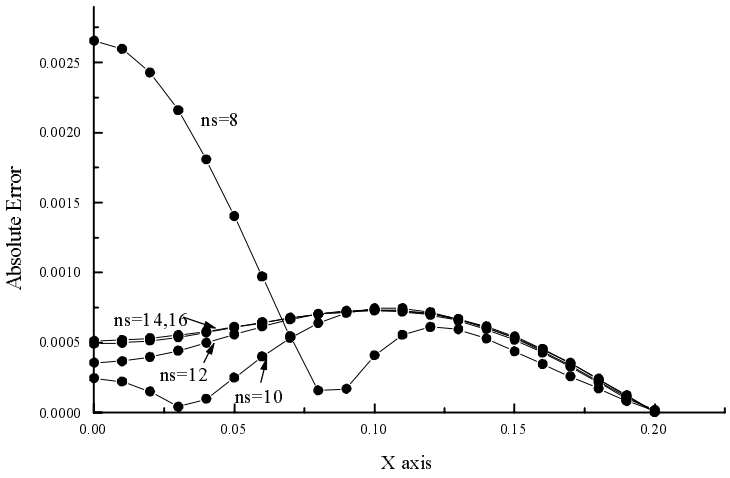

Figure 19. Comparison of errors for the diffusion equation in 2D.

We observe that LTDRM and LTMFS errors in Fig. 19 are basically identical. This implies that the interpolation errors for finding particular solutions in the LT space are negligible in this example. This is consistent with the theoretical analysis given in Section 4.3.

In LT space the forcing term of the modified Helmholtz's equation is $1/k$, a constant. The TPS with augmented linear term approximates $1/k$ exactly. Furthermore, $\Psi(r)$ in Eqn. (212) can be evaluated analytically. In contrast to the LTDRM in [24], the forcing term of the Laplacian can not be interpolated exactly. Another reason that our results are superior to those in [24, 82] is that the dominant part of the computational error in [24, 82] may be due to low convergence rate of the BEM [72].

Following Example 5.3.1.3 we will compare the CPU times of the current method and Example 5.2.1.2.

Example 5.3.1.3 We implemented our version of the LTDRM for the problem in Example 5.2.1.2. Again, the collocation and source points of the MFS are chosen in the same fashion as in Example 5.2.1.2.

To interpolate the forcing term, we chose 30 quasi-random points inside the cube. The results, as shown in Fig. 20, exhibited similar behavior to that in Example 5.3.1.2. The notation in Fig. 20 is defined in the similar way as in Fig. 19. Again, there is practically no difference between the LTMFS and the LTDRM as shown in Fig. 20.

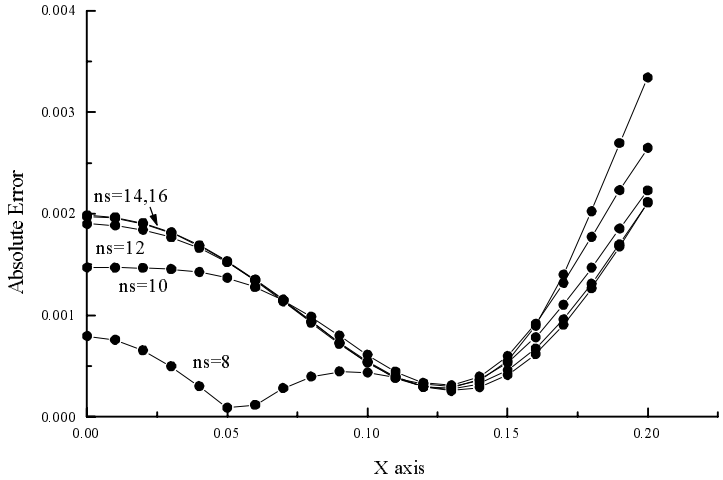

Figure 20. Comparion of errors for the diffusion equation in 3D.

Table 9 illustrates the efficiency of our approach. We used the same computer as for the computations in Examples 5.3.1.2 and 5.3.1.3. In Table 9, we notice little difference in CPU times. Our approach is especially attractive for 3D problems.

Table 9. CPU times for an interior point in Examples 5.3.1.2 and 5.3.1.3.

n_s	CPU (seconds)	
	2D	3D
8	0.99	1.32
10	1.16	1.54
12	1.37	1.81
14	1.52	2.14
16	1.76	2.41

6 Conclusions

In this chapter we have surveyed some recent theoretical and computational developments in the MFS. In particular, we have shown how to extend the method to solve inhomogeneous, nonlinear and time-dependent problems. In the past, the MFS has been used primarily to solve homogeneous elliptic problems. We have discussed some convergence and stability results of Katsurada, Okamoto and Kitigawa for Laplace's equation in $\mathbb{R}^2$ which shed new light on the convergence and stability properties of the method. Some of these results are extended to establish the convergence of MFS-RBF algorithms for Poisson's equation which corroborate the results of numerical experiments. The use of the Laplace transform in conjuction with the MFS-RBF method provides efficient algorithms for the solution of diffusion problems in $\mathbb{R}^2$ and $\mathbb{R}^3$.

Although the MFS has been in existence for over 30 years, we believe it is underutilized and much remains to be done, in particular with respect to convergence analysis for problems in $\mathbb{R}^3$. In future work we expect to extend the method to solve systems of nonlinear PDEs, equations with nonconstant coefficients and applications to problems with non-traditional boundary conditions. We hope the reader will be encouraged to develop further theory and applications.

Acknowledgment The second author acknowledges sabbatical support from the University of Nevada, Las Vegas and partial support from Professor C.A. Brebbia at Wessex Institute of Technology, U.K., during his sabbatical leave (1996-1997). The second author also acknowledges partial support of a collaborative research grant from NATO under reference CRG 970593.

References

[1] Partridge, P.W., Brebbia, C.A. & Wrobel, L.C., *The Dual Reciprocity Boundary Element Mehod*, Computational Mechanics Publications, Southampton and Elsevier, London, 1992.

[2] Golberg, M.A. & Chen, C.S., *Discrete Projection Methods for Integral Equations,* Computational Mechanics Publications, Southampton, 1996.

[3] Mackerle, J., Some remarks on progress with boundary elements, *Boundary Elements Communications*, **5**, 1-5, 1994.

[4] Atkinson, K.E. & Chien, D., Piecewise polynomial collocation for boundary integral equations, *SIAM Journal on Scientific and Statistical Computing*, **76**, 651-681, 1985.

[5] Sauter, S.A. & Krapp, A., On the effect of numerical integration in the Galerkin boundary element method, *Numerische Mathematik*, **74**, 337-360, 1996.

[6] Wearing, J.L. and Betahar, O., The analysis of plate bending problems using the regular direct boundary element method, *Engineering Analysis with Boundary Elements*, **16**, 261-271, 1995.

[7] Johnston, R.L. & Fairweather, G., The method of fundamental solutions for problems in potential flow, *Applied Mathematical Modelling*, **8**, 265-270, 1984.

[8] Karageorghis, A. & Fairweather, G., The method of fundamental solutions for the solution of nonlinear plane potential problems, *IMA Journal of Numerical Analysis*, **9**, 231-242, 1989.

[9] Karageorghis, A. & Fairweather, G., The method of fundamental solutions for the numerical solution of the biharmonic equation, *Journal of Computational Physics*, **69**, 435-459, 1987.

[10] Golberg, M.A. & Chen, C.S., On a method of Atkinson for evaluating domain integrals in the boundary element method, *Applied Mathematics and Computation*, **60**, 125-138, 1994.

[11] Golberg, M.A., Chen, C.S. & Karur, S.R., Improved multiquadric approximation for partial differential equations, *Engineering Analysis with Boundary Elements*, **18**, 9-17, 1996.

[12] Chen, C.S., The method of fundamental solutions for non-linear thermal explosions, *Communications in Numerical Methods in Engineering*, **11**, 675-681, 1995.

[13] Koopman, G.H., Song, L. & Fahnline, J.B., A method for computing acoustic fields based on the principle of wave superposition, *Journal of Acoustical Society of American*, **86**, 2433-2438, 1988.

[14] Cao, Y., Schultz, W. & Beck, R., Three dimensional desingularized boundary integral methods for potential problems, *International Journal for Numerical Methods in Engineering*, **12**, 785-803, 1991.

[15] Amano, K., A charge simulation method for the numerical conformal mapping of interior, exterior and doubly connected domains, *Journal of Computational and Applied Mathematics*, **53**, 353-370, 1994.

[16] Chen, C.S. & Golberg, M.A., Las Vegas method for diffusion equations, *Boundary Element Technology XII*, eds. J.I. Frankel, C.A. Brebbia & M.A.H. Aliabadi, Computational Mechanics Publications, 299-308, 1997.

[17] Katsurada, M. & Okamoto, H., A mathematical study of the charge simulation method, *Journal of the Faculty of Science, University of Tokyo, Section 1A*, **35,** 507-518, 1988.

[18] Katsurada, M., Asymptotic error analysis of the charge simulation method in a Jordan region with an analytic boundary, *Journal of the Faculty of Science of Tokyo University, Section 1A*, **37**, 635-657, 1990.

[19] Cheng, R.S.C., *Delta-Trigonometric and Spline Methods using the Single-Layer Potential Representation*, Ph.D. dissertation, University of Maryland, 1987.

[20] Kitagawa, T., On the numerical stability of the method of fundamental solutions applied to the Dirichlet problem, *Japan Journal of Applied Mathematics*, **35**, 507-518, 1988.

[21] Kitagawa, T., Asymptotic stability of the fundamental solution method, *Journal of Computational and Applied Mathematics*, **38**, 263-269, 1991.

[22] Bogomolny, A., Fundamental solutions method for elliptic boundary value problems, *SIAM Journal on Numerical Analysis*, **22**, 644-669, 1985.

[23] Amini, S., Harris, P.J. & Wilton, D.J., *Coupled Boundary and Finite Element Methods for the Solution of Dynamic Fluid-Structure Interaction Problem*, Lecture Notes in Engineering, eds. C.A. Brebbia and S.A. Orszag, Springer-Verlag, Berlin, 1992.

[24] Zhu, S., Satravaha, P. & Lu, X., Solving Linear Diffusion Equations with the Dual Reciprocity Method in Laplace Space, *Engineering Analysis with Boundary Elements*, **13**, 1-10, 1994.

[25] Pasquetti, R., Caruso, A. & Wrobel, L.C., Transient problems using time-dependent fundamental solutions, *Boundary Element Methods in Heat Transfer*, eds. L.C. Wrobel and C.A. Brebbia, Computational Mechanics Publications, Southampton, 1992.

[26] Golberg, M.A. & Chen, C.S. and Rashed, Y.F., The annihilator method for computing particular solutions to partial differential equations, submitted for publication.

[27] Strang, G. & Fix, G.J., *An Analysis of the Finite Element Method*, Prentice-Hall, Englewood Cliffs, 1973.

[28] Atkinson, K.E., A discrete Garlerkin method for first kind integral equations with a logarithmic kernel, *Journal of Integral Equations and Applications*, **1**, 343-363, 1988.

[29] Chen, Y. & Atkinson, K.E., *Solving a Single Layer Integral Equation on Surfaces in* $\mathbb{R}^3$, The University of Iowa, Department of Mathematics, Technical Report, No. 51, 1994.

[30] Klees, R., Gravity field determination using boundary element methods, *Surveys in Geophysics*, **14**, 419-432, 1993.

[31] Freeden, W. & Kersten, H., A constructive approximation theorem for the oblique derivative problem in potential theory, *Mathematical Methods in Applied Science*, **3**, 104-114, 1981.

[32] Christiansen, S. & Sararen, J., The conditioning of some numerical methods for first kind integral equations, *Journal of Computational and Applied Mathematics*, **67**, 43-58, 1996.

[33] Christiansen, S. & Hansen, P.C., The effective condition number applied to error analysis of certain boundary collocation methods, *Journal of Computational and Applied Mathematics*, **54**, 15-36, 1994.

[34] Han, P.S., Olsen, M.D. & Johnson, R.L., An adaptive boundary element method, *International Journal for Numerical Methods in Engineering*, **24**, 1187-1202, 1987.

[35] Atkinson, K.E., A survey of boundary integral equation methods for the numerical solution of Laplace's equation in three dimensions, Chapter 1, *Numerical Solution of Integral Equations*, ed. M.A. Golberg, Plenum, New York, 1990.

[36] Amini, S. & Sloan, I., Collocation methods for second kind integral equations with non-compact operators, *Journal of Integral Equations and Applications*, **2**, 1-30, 1989.

[37] Babuska, I. & Suri, M., The p and $h-p$ versions of the finite element method, basic principles and properties, *SIAM Review*, **36**, 307-347, 1994.

[38] Karageorghis, A., Modified methods of fundamental solutions for harmonic and biharmonic problems with boundary singularities, *Numerical Methods for Partial Differential Equations*, **8**, 1-19, 1992.

[39] Poullikkas, A., Karageorghis, A. & Georgiou, G., Method of fundamental solutions for harmonic and biharmonic boundary value problems, *Computational Mechanics*, to appear.

[40] Kress, R., A Nyström method for boundary integral equations with corners, *Numerische Mathematik*, **58**, 145-161, 1990.

[41] Kupradze, V.D. & Aleksidze, M.A., The method of functional equations for the approximate solution of certain boundary value problems, *U.S.S.R. Computational Mathematics and Mathematical Physics*, **4**, 82-126, 1964.

[42] Katsurada, M. & Okamoto, H., The collocation points of the fundamental solution method for the potential problem, *Computers and Mathematics with Applications*, **31**, 123-137, 1996.

[43] Ahlfors, L.V., *Complex Analysis, An Introduction to the Theory of Analytic Functions of One Complex Variable*, McGraw-Hill, New York, 1953.

[44] Katsurada, M., Charge simulation method using exterior mapping functions, *Japan Journal of Industrial and Applied Mathematics*, **11**, 47-61, 1994.

[45] Arnold, D.N. & Wendland, W.L., The convergence of spline collocation for strongly elliptic equations on curves, *Numerische Mathematik*, **47**, 317-341, 1985.

[46] Dongarra, J.J., *Linpack Users Guide*, SIAM, Philadelphia, 1979.

[47] Chan, T.F. & Foulser, D., Effectively well-conditioned linear systems, *SIAM Journal of Scientific and Statistical Computing*, **9**, 963-969, 1988.

[48] Geng, P., Oden, J.T. & Demkowicz, L., Numerical solution and a posteriori error estimation of exterior acoustics problems by a boundary element method at high wave numbers, *Journal of the Acoustical Society of America*, **100**, 335-345, 1996.

[49] Pollandt, R., Solving nonlinear equations of mechanics with the boundary element method and radial basis functions, *International Journal for Numerical Methods in Engineering*, **40**, 61-73, 1997.

[50] Golberg, M.A. & Chen, C.S., The theory of radial basis functions applied to the BEM for inhomogeneous partial differential equations, *Boundary Elements Communications*, **5**, 57-61, 1994.

[51] Brebbia, C.A. & Nardini, D., Dynamic analysis in solid mechanics by an alternative boundary element procedure, *Solid Dynamics and Earthquake Engineering*, **65**, 147-164, 1983.

[52] Atkinson, K.E., The numerical evaluation of particular solutions for Poisson's equation, *IMA Journal of Numerical Analysis*, **5**, 319-338, 1985.

[53] Cheng, A.H.D., Grilli, S. & Lafe, O., Dual reciprocity BEM based on complete global shape functions, *BEM XVII*, Computational Mechanics, Southampton, 1995.

[54] Golberg, M.A. & Chen, C.S., A bibliography on radial basis function approximation, *Boundary Elements Communications*, **7**, 155-163, 1996.

[55] Powell, M.J.D., The theory of radial basis function approximation in 1990, *Advances in Numerical Analysis, Vol II*, ed. W. Light, Oxford Science Publications, Oxford, 1992.

[56] Duchon, J., Splines minimizing rotation invariant semi-norms in Sobolev spaces, In *Constructive Theory of Functions of Several Variables*, Lecture Notes in Mathematics 571, ed. W. Schempp & K. Zeller, Springer-Verlag, Berlin, 85-110, 1976.

[57] Madych, W.R., Miscellaneous error bounds for multiquadric and related interpolants, *Computers and Mathematics with Applications*, **24**, 121-138, 1992.

[58] Hardy, R.L., Multiquadric equations of topography and other irregular surfaces, *Journal of geophysical Research*, **176**, 1905-1915, 1971.

[59] Franke, R., Scattered data interpolation: tests of some methods, *Mathematics of Computation*, **48**, 181-200, 1982 .

[60] Powell, M.J.D., The uniform convergence of thin plate spline interpolation in two dimensions, *Numerische Mathematik*, **68**, 228-255, 1994.

[61] Levesley, J., *Pointwise Estimates for Multivariate Interpolation Using Conditionally Positive Definite Functions*, University of Leicester, 1994.

[62] Kansa, E.J., Multiquadrics - A scattered data approximation scheme with applications to computational fluid-dynamics (I), *Computers and Mathematics with Applications,* 1990, **19**, 127-145.

[63] Hon, Y.C. & Mao, X.Z., An efficient numerical scheme for Burger's equation, to appear in *Applied Mathematics and Computation.*

[64] Hon, Y.C., Lu, M.W., Xu, W.M. & Zhu, Y.M., Multquadric method for the numerical solution of a biphasic mixture model, to appear in *Applied Mathematics and Computation.*

[65] Beatson, R.K. & Powell, M.J.D., Univariate interpolation on a regular finite grid by a multiquadric plus a linear polynomial, *IMA Journal of Numerical Analysis*, **12**, 107-137, 1992.

[66] Milroy, M.J., Vickers, G.W. & Bradley, C., An adaptive radial basis function approach to modelling scattered data, preprint, 1994.

[67] Chan, C.Y. & Chen, C.S., The method of fundamental solutions for multiple dimensional quenching problems, *Proceedings of Dynamic Systems and Applications*, **2**, 115-122, 1996.

[68] Chan, C.Y., Computation of the critical domain for quenching in an elliptic plate, *Neural and Parallel Scientific Computing,* **1**, 153-162, 1993.

[69] Chen, C.S. & Golberg, M.A., A domain embedding method and the quasi-Monte Carlo method for Poisson's equation, *Boundary Elements XVII*, eds. C.A. Brebbia, S.Kim, T.A. Osswald, H. Power, Computational Mechanics Publications, 115-122, 1995.

[70] Niederreiter, H., *Random Number Generation and Quasi-Monte Carlo Methods*, SIAM, CBMS 63, Philadelphia, PA, 1992.

[71] Golberg, M.A., The method of fundamental solutions for Poisson's Equation, *Engineering Analysis with Boundary Elements,* **16**, 205-213, 1995.

[72] Golberg, M.A., Chen, C.S., Bowman, H. & Power, H., Some comments on the use of radial basis functions in the dual receprocity method, to appear in *Computational Mechanics.*

[73] Miranda, C., *Partial Differential Equations of Elliptic Type*, Springer-Verlag, New York, 1970.

[74] Schaback, R., Error estimates and condition numbers for radial basis function interpolation, *Advances in Computational Mathematics*, **3**, 251-264, 1995.

[75] Jeon, Y. & Atkinson, K.E., *An Integral Equation Program for the Planar Laplace Equation*, Mathematics Department, University of Iowa, Iowa city, 1993.

[76] Karur, S.R. & Ramachandran, P.A., Augmented thin plate spline approximation in DRM, *Boundary Elements Communications*, **6**, 55-58, 1995.

[77] Agnantiaris, J.P., Polyzos, O. & Beskos, D.E., Some studies on the dual reciprocity BEM for elastodynamic analysis, *Computational Mechanics*, **17**, 270-277, 1996.

[78] DeMey, G., The auxilliary boundary element method for time dependent problems, *Journal of Computational and Applied Mathematics*, **12-13**, 239-245, 1985.

[79] Walker, S.P., Diffusion problems using transient discrete source superposition, *International Journal of Numerical Methods in Engineering*, **35**, 165-178, 1997.

[80] Rizzo, F. & Shippy, D.J.A., A Method of Solution for Certain Problems of Transient Heat Conduction, *AIAA Journal*, **8,** 2004-2009, 1970.

[81] Stehfest, H., Algorithm 368: Numerical Inversion of the Laplace Transform, *Communincations of the ACM*, **13**, 47-49**,** 1970.

[82] Moridis, G.L. & Reddell, D.L., The Laplace Transform Boundary Element (LTBE) Method for the Solution of Diffusion-type Equations, *Boundary Elements XIII*, Vol. 1, Springer-Verlag, Berlin, 83-97, 1991.

[83] Satravaha, P., *Solving Linear and Nonlinear Transient Diffusion Problems with the Laplace Transorm Dual Reciprocity Method*, Ph.D. Thesis, Department of Mathematics, The University of Wollongong, Wollongong, Australia, 1996.

[84] Zhu, S. & Satravaha, P., An efficient computational method for modelling transient heat conduction with nonlinear source terms, *Applied Mathematical Modelling,* **20,** 513-522, 1996.

[85] Zhu, S., Particular solutions associated with the Helmholtz operator used in DRBEM, *Boundary Element Abstracts*, **4**, 231-233, 1993.

[86] Chen, C.S. & Rashed, Y.F., *Evaluation of Thin Plate Sline Based Particular Solutions for Helmholtz-type Operator for the DRM*, Department of Mathematical Sciences, 97–06, University of Nevada, Las Vegas, U.S.A.

[87] Abramowitz, M. & Stegun, I.A., *Handbook of Mathematical Functions*, Dover, New York, 1965.

[88] Carslaw, H.S. & Jaeger, J.C, *Conduction of Heat in Solids*, Oxford University Press, London, 1959.

[89] W.R. Derrick & S.I. Grossman, *Elementary Differential Equations with Applications*, Addison-Wesley Publishing Co., 1976.